Universidad
Carlos III de Madrid
www.uc3m.es

TITLE

ELECTRIC FIELDS ON COLLECTIVE CELL MIGRATION IN EPITHELIAL CELL MONOLAYERS

AUTHOR: JUAN MANUEL CASTRO GÓMEZ

TUTOR: LETICIA VALENCIA BLANCO

DATE: JULY-07-2014

BACHELOR THESIS

BIOMEDICAL ENGINEERING

AGRADECIMIENTOS

A mis padres, mi hermana, mis tíos y demás familia que se ha interesado por este proyecto, ayudándome de las más inimaginables y diversas maneras.

A todos los técnicos de los numerosos laboratorios que he recorrido mientras he estado haciendo experimentos, por su ayuda y sus consejos. Especialmente a Angélica que se ha preocupado porque las cosas me salieran bien a pesar de mi empeño por lo contrario.

A Javi por proponerme este proyecto y, sobre todo, a Leticia, por todo lo que me ha ayudado y aguantado.

Muchas gracias a todos.

ABSTRACT

Endogenous electric fields induced during wound healing seem to be one of the most relevant cues for the process. It has also been observed that the induction of external fields affects wound healing usual performance. However, the electric behavior of wounds has not been quantitatively modeled yet in a precise way. The current work is focused on the study in keratinocyte monolayers of both, electrical signaling after injury and cell behavior under the effect of induced electric fields. The results show that potential differences are generated during wound healing of keratinocyte monolayers, being the potential higher inside the wound than in the cellular region. Regarding voltage induction, the cell behavior is affected by the potential difference produced, being the range from 0 to 150 mV the most interesting for reepithelialization enhancement. This project is aimed to be the starting point of a much bigger one: the design of a device to control skin behavior during wound healing. Now, such a complex objective is still very far away, but the results lead to believe that it is an achievable goal.

TableOfContents

ListOfFigures

ListOfFigures

1. INTRODUCTION

1.1. SKIN

Although many people might not think about skin as an organ, it is, in fact, the largest organ of the body. Skin covers all the surface of human body and it is the primary and principal site of interaction with the environment. Within its functions are found: the protection of internal tissues against ultraviolet sunrays, pathogenic microorganisms, fluid loss and mechanical, chemical and thermal stresses; metabolic functions such as production of vitamin D and triglycerides; sensory perception of touch, temperature, pressure and pain; and regulation of temperature. Skin has an area of about 2 m^2 and it weights around 5 kg (7% of the body weight) in an average adult. Its thickness usually ranges from 1 to 2 mm, but it can be as thin as 0.5 mm (on the eyelids) or as thick as 4 mm (on the palms of the hands and the soles of the feet). But skin thickness not only varies among anatomical location, it also depends on facts such as age (children have thinner skin, which thickens until the individual reaches 50 to 60 years old, when it starts to reduce in thickness again) and sex of the individual (female skin is typically thinner than male skin all over the body). [1,2]

The skin is divided in two layers: epidermis and dermis. A third subcutaneous layer, called hypodermis, is found underneath the dermis (figure 1.1). The epidermis is the outermost layer of the skin. It is an avascular structure, so the cells need to receive the nutrients via diffusion from the dermis. Four different types of cells form the epidermis: keratinocytes, which are the major cells (almost 90%), produce keratin, a protein that makes them tough and water-resistant; melanocytes, in charge of producing melanin, a protein that absorbs radiant energy; Lagerhans cells, which are involved in the immune response; and Merkel cells, specialized in light touch sensation. Its structure is composed of 40 to 50 rows of cells, divided in four layers, which are, from the inside to the outside: stratum basal, stratum spinosum, stratum granulosum, and stratum corneum. The keratinocytes in outer layers are in further steps of differentiation than the ones from the inner layers. The cells from the basal layer are continuously reproducing and pushing older cells towards the surface. The outermost rows are composed of death cells that will finally detach. It typically takes about two weeks for a cell to reach the outer layers and die, and two more weeks to peel off.

The dermis is deeper and thicker. It is subdivided in two regions: the papillary layer and the reticular layer. The dermis contains skin accessory structures: hair, sweat and sebaceous glands, nervous fibers and blood vessels. The major cell type is the fibroblast, which produce collagen and elastic fibers, the essential components of the dermis, and give it the characteristic strength and resistance. The underlying layer, the hypodermis, is essentially composed of adipose tissue that serves as fat storage, thermal insulator and flexible connection between skin and underlying structures.

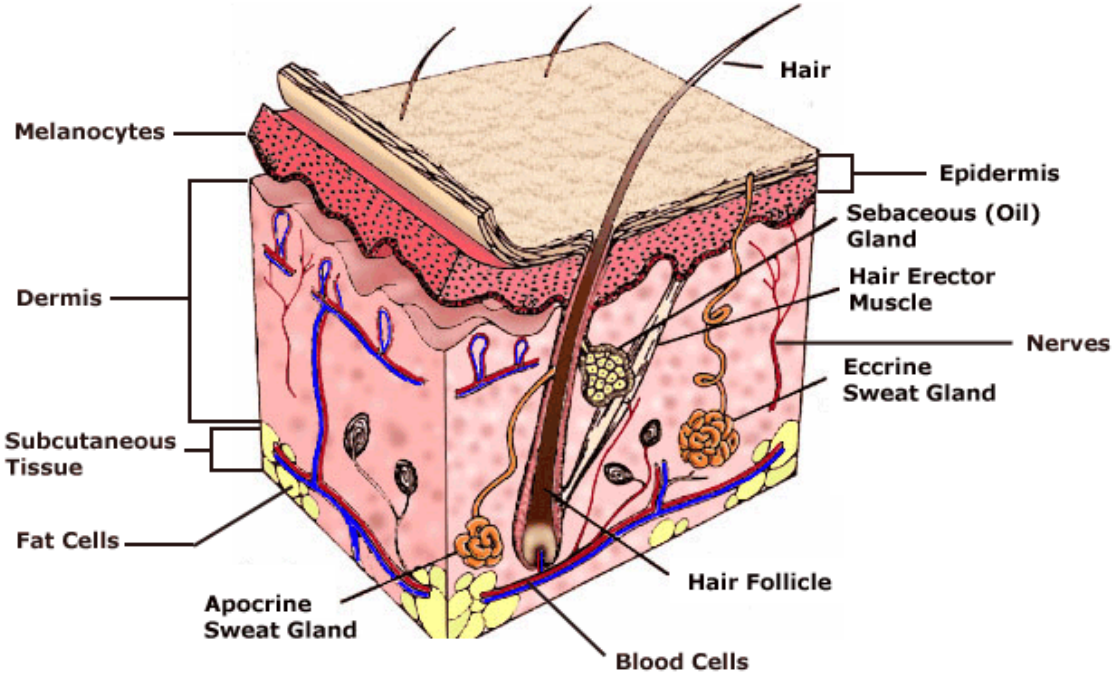

Figure 1.1. The structure of skin.

1.2. WOUND HEALING

Wound healing is a complex and dynamic process that consists on replacing death or missing tissue and cellular structures. Wound healing is the natural regenerative response of the body to tissue injury. The interaction of a complex cascade of cellular events restores the tensile strength and characteristics of the injured tissue. As skin is the protective barrier against the outside world, any break in it must be rapidly and efficiently repaired. The wound healing is a process that is usually divided into four different phases: hemostasis, inflammation, granulation and maturation. However, wound healing is a very complex process and these phases are highly integrated and overlapped. For wound healing to develop properly, it is necessary that they take place in the proper sequence, start at a concrete time, last a specific duration and have an optimal intensity.

Right after injury, there exist an outflow of blood and lymphatic fluid. The initial hemostasis phase starts immediately, limiting blood loss. In the beginning, vasoactive mediators induce vasoconstriction, reducing the blood income to the injured area. Platelets aggregate and adhere to the damaged zone, forming a clot. Platelet-derived growth factor (PDGF), proteases and vasoactive agents are released. Thrombocytes are attracted to the wound and blood vessels dilate to allow more blood income now that blood loss has been avoided.

The inflammatory phase starts with the arrival of neutrophils, overlapping with the hemostasis phase. Transforming growth factors (TGF) are released to attract

neutrophils. These cells, which are in charge of cleaning bacteria and death tissue from the wound, are the predominant type during the first part of the process (24-48 hours). But they are not the essential cell for wound healing, the most important cells are macrophages, which phagocyte debris and bacteria and release many important factors affecting the wound healing process. T lymphocytes, which secrete lymphokines and play a key role in the immune response, arrive to the injury later (72 hours), but still during the inflammatory phase.

The granulation phase is usually subdivided in fibroplasia, collagen matrix deposition, angiogenesis and contraction or reepithelialization. Fibroblasts are critical for granulation tissue, as they are the cells that produce collagen. Collagen is secreted in the extracellular space in the form of procollagen, which aggregate to form collagen filaments. Within the collagen matrix new blood vessels are formed to increase blood flow to the wound, so more healing factors are available and perfusion is improved. Finally, wound contraction, the closure of wound edges by migration of epithelial cells, induce a decrease in wound size.

The ultimate phase, called maturation or remodeling, involves essentially an increase in collagen organization. The third week after injury, collagen is degraded and deposited in an increasingly organized structure. The maximum tensile strength of a scar after healing only reaches about 80 % the tensile strength of healthy skin. [3,4]

1.3. ELECTRIC POTENTIAL AND FIELDS IN SKIN

It has been widely studied that cells maintain a voltage across their plasma membranes. This voltage is used in many different ways, for example, coupled transport of molecules through the membrane, rapid signaling from cell surface and long distance communication as in the case of neurons. Scaling up to the multicellular domain, we find similar behavior. The same way a cell is surrounded by a plasma membrane, every organ is surrounded by an epithelium and, actually, the largest organ in our bodies, the skin, is a multi-layered epithelium. However, in contrast to the attention paid to the electrical properties of the plasma membrane, those of the epithelia are barely mentioned. The epithelium can be considered to the organ as the plasma membrane to the cell, both determine what can go in and out of the structure that they protect inside. Analogous to the cellular membrane, epithelia produce a voltage across the epithelial layer. The intensity of this voltage in humans skin has been observed to be about 10mV to 60mV, positive inside, depending on the region measured [5]. What is more, this transepithelial potential (TEP) is present in many other types of epithelia, not only in the skin [6,7,8].

Once the existence of TEP is known, the next step is wondering what happens when it is broken, i.e. a wound. There are measurements of electrical phenomena associated with wounds as early as mid XIX century. In 1843, DuBois-Reymond measured a current of about 1 μA in a cut in one of his fingers [9]. More modern techniques have been used to

measure currents as large as 100 μA/cm^2 in the stumps of regenerating newt limbs [10]. In humans, similar measurements have been performed on fingertip amputation, observing up to 30 μA/cm^2 currents that leave the stump for about three weeks after injury [11]. Based on human tissue resistivity, these currents would generate an electric field of 10-100 mV/mm. Spatially, the strongest currents are found at the wound edge; with wound center having lower values. Temporally, skin wounds present currents that slowly rise to a peak in about 120 min (figure 1.2) [12,13]. The slow increase and reversal of the currents make think that the wound electric behavior is an active response: for the current to be a passive leakage phenomena (thinking about the wound as a short circuit of TEP), it should have risen to the peak immediately after injury [14].

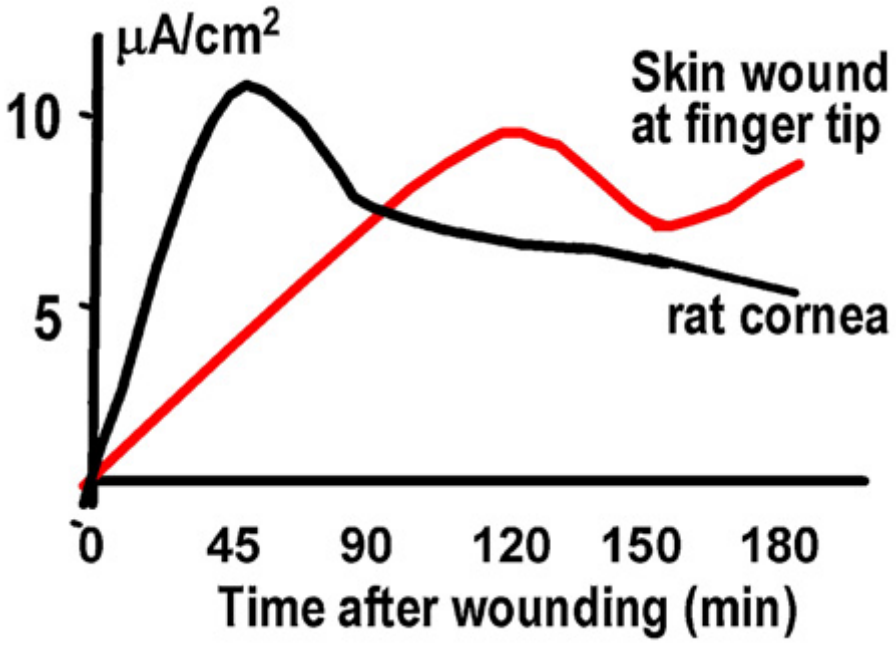

Figure 1.2. Endogenous wound electric currents at skin and cornea wounds.

Until now, the electric observation has been presented as current measurements. Nevertheless, tissue resistivity can vary depending on cell density and structural anatomy, so potential measurements need to be taken directly for reliability. The typical range of field strengths has been found to be between 40 and 200 mV/mm. Another important point is the field direction, discovered to be a function of position. Below the epidermis the field is more negative at the wound center (fibroblasts affected by this pole orientation), but above the epidermis the electric poles are inverted, so the wound center has a higher potential (keratinocytes, thus, would move on the opposite direction to fibroblasts under the same field) (figure 1.3). Although a known occurring phenomena, no accurate quantitative modeling has been yet performed on electric behavior of wounds. [15]

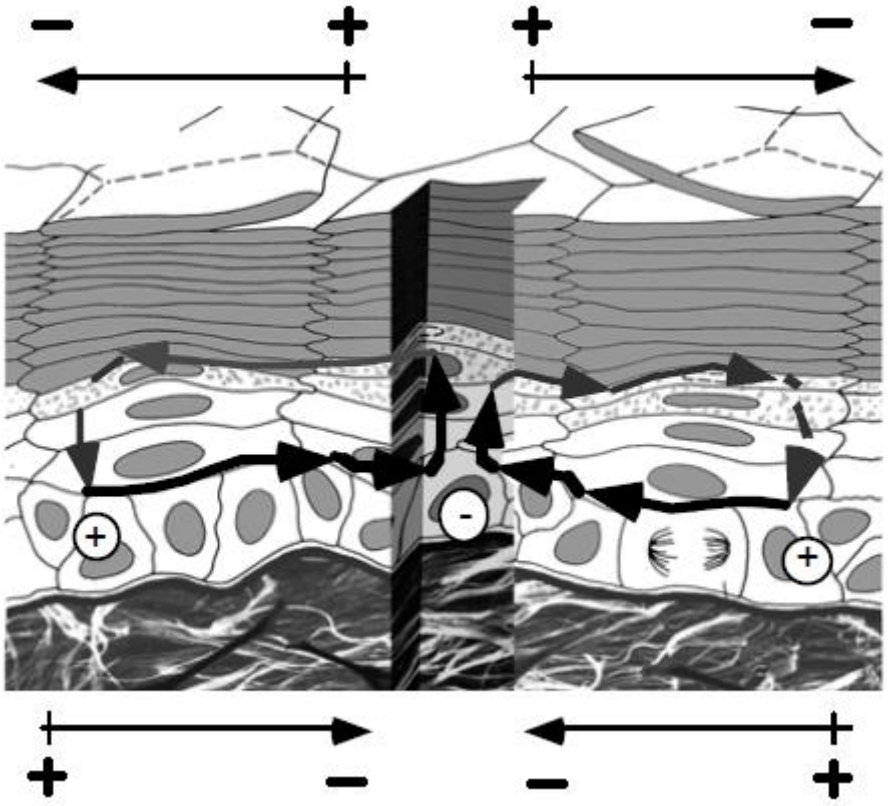

Figure 1.3. Generation of wound electric fields. After injury, the potential produce a current flow through the low resistance path generated. The lateral electric field induced at the lower layers is more negative in the wound center while the upper portion is more positive inside.

Now we know that endogenous electric fields are naturally present in wounds. The next step would be to determine the importance of electric fields in wound healing. The role of electric field was firstly investigated in frog embryos. The result indicated that wound healing requires endogenous electric currents, which supports the important role of electric fields in wound healing [16]. A new attempt was performed on small skin wound in both, the right and left foot of newts [17]. They monitored the healing rate while changing the lateral electric field near the wounds. The wounds with enhanced electric field healed faster than the ones without field. The results seem to be consistent with the hypothesis established about the endogenous electric fields in wounds, which states that they promote epithelialization. Later experiments showed that an increase in electric field derived from injury enhanced epithelialization and a decrease in the electric field significantly retarded the process [14,18].

2. OBJECTIVES AND ORGANIZATION

The final aim behind the present work would be the implementation of a device able to control the superficial evolution of wounds, more concretely, the skin behavior during wound healing. After some research on current bibliography, it has been observed that a key point on the cellular movements of the skin after injury is related to electric phenomena [14,19]. Thus, the device design would be based on the control that applied electromagnetic fields might have on wound healing. The project is clearly a multidisciplinary job that will encompass very distinct fields such as electronics, programming, cell biology or tissue engineering.

However, the main objective is a long term proposal, which may be achievable after several research steps. As explained before, wound healing is a very complex process, affected by many factors. To study the problem, it should be initially simplified. Thus, the initial work will consist on the analysis of the behavior of cellular monolayers after injury. The use of monolayers makes necessary to distinguish between the two layers that compose the skin: an outer one composed by keratinocytes and an inner layer of fibroblasts. The research that will be presented within this work is related to the study of electrical signaling after injury in keratinocyte monolayers and the behavior of such monolayers under the effect of induced electric fields. Next step would be to perform similar analysis on fibroblast monolayers. After monolayers have been studied separately, a 3D configuration bilayer, composed of both keratinocytes and fibroblasts, would be necessary to observe the effect of electric fields more accurately. Based on the results obtained in previous steps, some studies in vivo would be performed and, ultimately, the device could be designed and tested.

As an initial preview, the organization for the experiments performed for the present work (the initial step of the complete project, the study of keratinocyte monolayers) was the following:

- Design and fabrication of measuring system
- Development of electric data acquisition program
- Experiments to measure the electric potential generated by keratinocytes after injury
- Software to analyze the measurements on potential
- Design and fabrication of potential inducing system (part of the measuring system was reused, as it fitted well)
- Development of imaging acquisition system
- Experiments to measure velocity of keratinocyte movement under electric fields
- Software to analyze the measurements on cell movement

3. MATERIALS AND METHODS

The cells used for the experiments were HaCaT keratinocytes from CIEMAT. These HaCaT keratinocytes belong to an immortalized cell line, which means that they keep reproducing after several cycles, unlike primary cell cultures, which have a certain lifespan.

The containers used were: 2 ml cryotubes from Fisherbrand (figure 3.1.C); 35 mm petri dish, p35 and 100 mm petri dish, p100 (figure 3.1.A) from Thermo Scientific BioLite; and 15 mL and 50 mL centrifuge tubes (figure 3.1.B) from Labbox.

Two different pipettes were used, an electric one for higher volumes with three tips to select depending on the volume 1 mL, 10 mL and 25 mL (figure 3.1.B); and a precision pipette for small volumes with two tips for 10 µL to 100 µL and 100 µL to 1 mL selection (figure 3.1.A). The vacuum filter units with Surfactant-Free Cellulose Acetate (SFCA) membrane (figure 3.1.C) were from Thermo Scientific Nalgene.

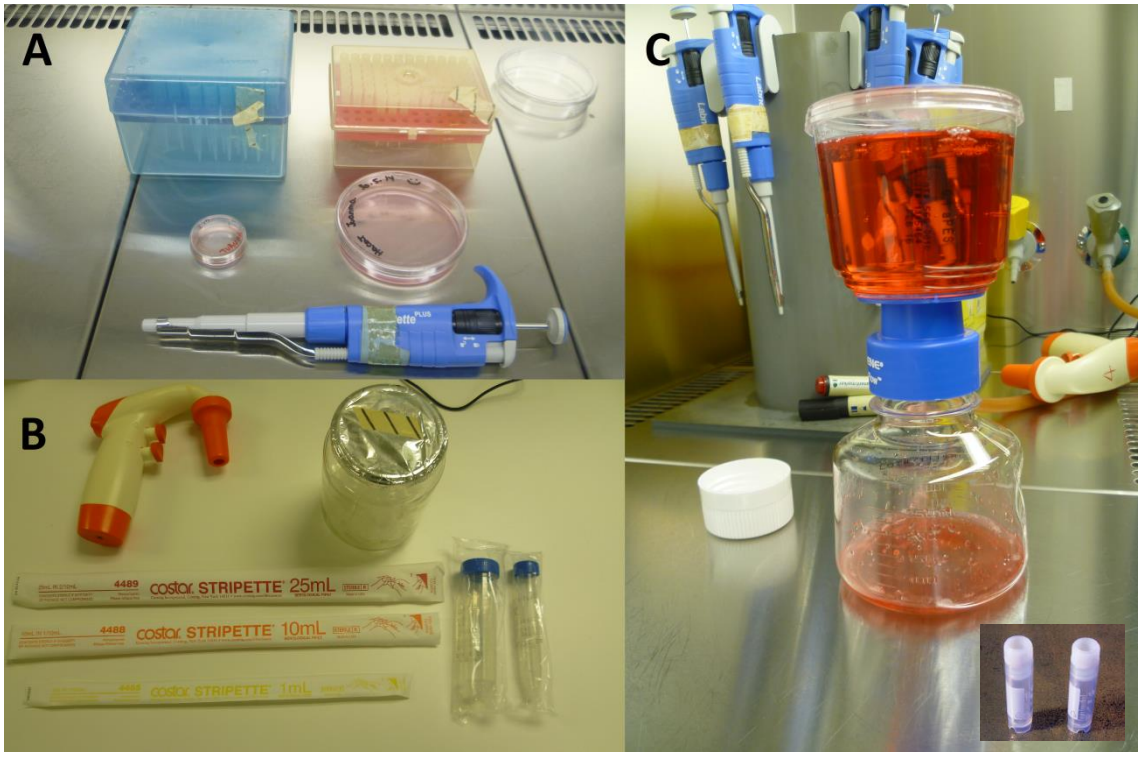

Figure 3.1. Containers, pipettes and filters. (A) Precision pippete (down) with tips for 10 µL to 100 µL (up, right) and 100 µL to 1 mL (up, left) and petri dishes, p35 (middle, left) and p100 (middle, right). (B) Electric pipette (up, left) with tips for 1 mL (yellow), 10 mL (orange) and 25 mL (red) and centrifuge tubes (down, right) 15 mL (rigth) and 50 mL (left). (C) Vacuum filter unit and 2 mL cryotubes (down, rigth).

Dulbecco's Modified Eagle Medium with high glucose content and without sodium pyruvate, DMEM, was from Invitrogen Gibco (figure 3.2.F). Fetal bovine serum, FBS, (figure 3.2.E) and the antibiotic/antimycotic solution (figure 3.2.A) were from Thermo

Scientific HyClone. The collagen from calf skin solution (figure 3.2.B) and the trypsine-EDTA solution (figure 3.2.D) were from SIGMA. The phosphate buffer saline, PBS, (figure 3.2.C) is prepared by the culture laboratories technician mixing 8 g (137 mM) of NaCl, 0.2 g (2.7 mM) of KCl, 1.44 g (10 mM) of NaHPO, 0.24 g (2mM) KHHPO and 800 mL of distilled water. Then, the pH is adjusted to 7.4 with HCl, the volume is set to 1 L with distilled water and the solution is autoclaved.

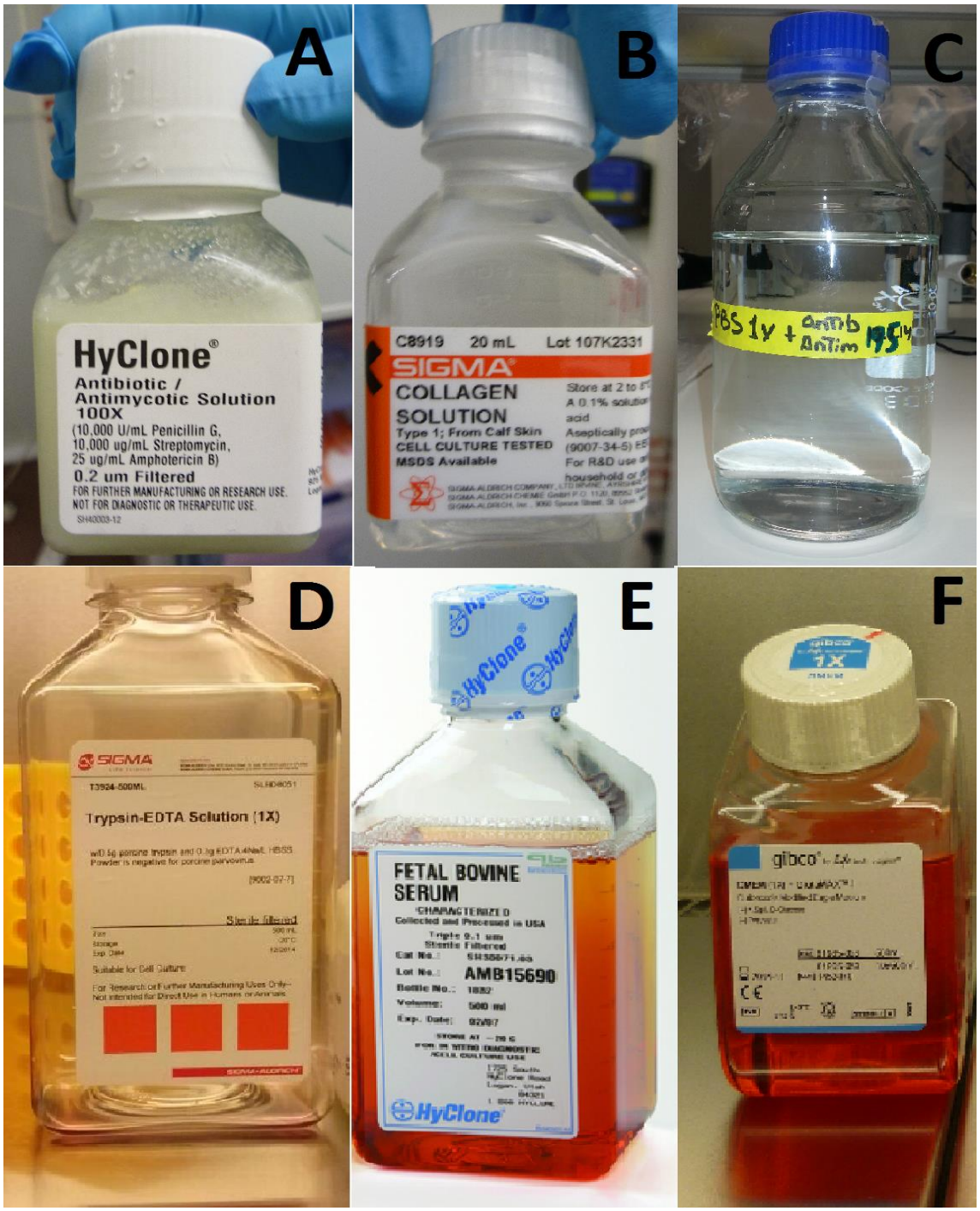

Figure 3.2. Laboratory reagents. (A) Antibiotic/Antimycotic solution. (B) Collagen solution. (C) Phosphate buffer saline. (D) Trypsine-EDTA solution. (E) Fetal bovine serum. (F) Dulbecco's Modified Eagle Medium

The necessary tools and machines used in the lab to work with the cells were: a Neubauer chamber (figure 3.3.A) to count the cells; vacuum chamber (figure 3.3.B) to remove the discarded solutions; safety waste cans (figure 3.3.C) for the biological waste; - 80 ºC freezer (figure 3.3.D) to keep the frozen cells; regular fridge with freezer (figure 3.3.E) to keep the medium and solutions; vertical laminar flux cabin (figure 3.3.F) where all the procedures were performed; two incubators to keep the cells at the right humidity conditions, 5% CO_2 concentration and 37 ºC, a big one where the petri dishes were usually placed (figure 3.3.G) and a small one for the petri dish with the scratch used during the observation under the microscope (figure 3.3.H); the centrifuge (figure 3.3.I) and the device for warm bath (figure 3.3.J).

Figure 3.3. Laboratory equipment. (A) Neubauer chamber. (B) Vacuum chamber. (C) Safety waste can. (D) – 80 ºC freezer. (E) Regular fridge. (F) Vertical laminar flux cabin. (G) Big incubator. (H) Small incubator. (I) Warm bath device. (J) Centrifuge.

The piece to hold the wires together and keep them on a specific place during measurements was made of tinted PVC (figure 3.4.A). It was fabricated by the fluid mechanics laboratories technician following a design which height matches exactly the distance between the base of the petri dish and its lid, 11 mm, and has four holes of 1 mm of diameter to put the wires inside (annex). Such design avoids the movement of the piece once it is placed inside the petri dish and it is properly stuck in the incubator with two metal holders. The wire was copper tinned AWG 30 with Teflon insulation. Four pieces of wire of approximately 25 cm long where stuck to the PVC structure using epoxy adhesive. A small hole was made on the p35 lid so the wires could go through (figure 3.4.C). For the measuring experiment one of the wires inside the petri dish might have to go to more than one input, so a wire clamp was used to split the signal (figure 3.4.B).

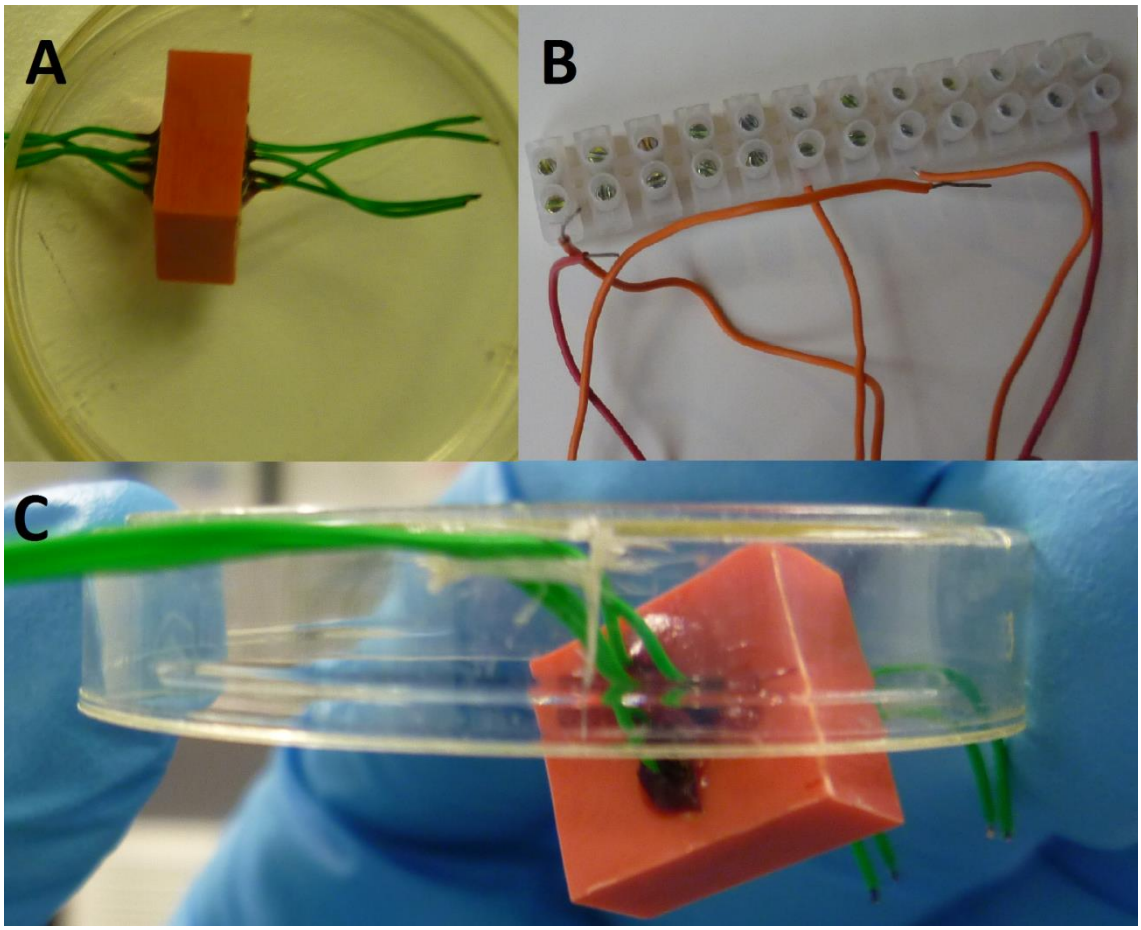

Figure 3.4. Wires and related structures. (A) Tinted PVC structure with the wires stuck using epoxy adhesive. (B) Wire clamp. (C) Wires going through a small hole in the p35 lid.

Two different electric devices were needed: a power supply (figure 3.5.A) to generate the potential for the induction experiments and a micro voltmeter (figure 3.5.B) for the measuring experiments.

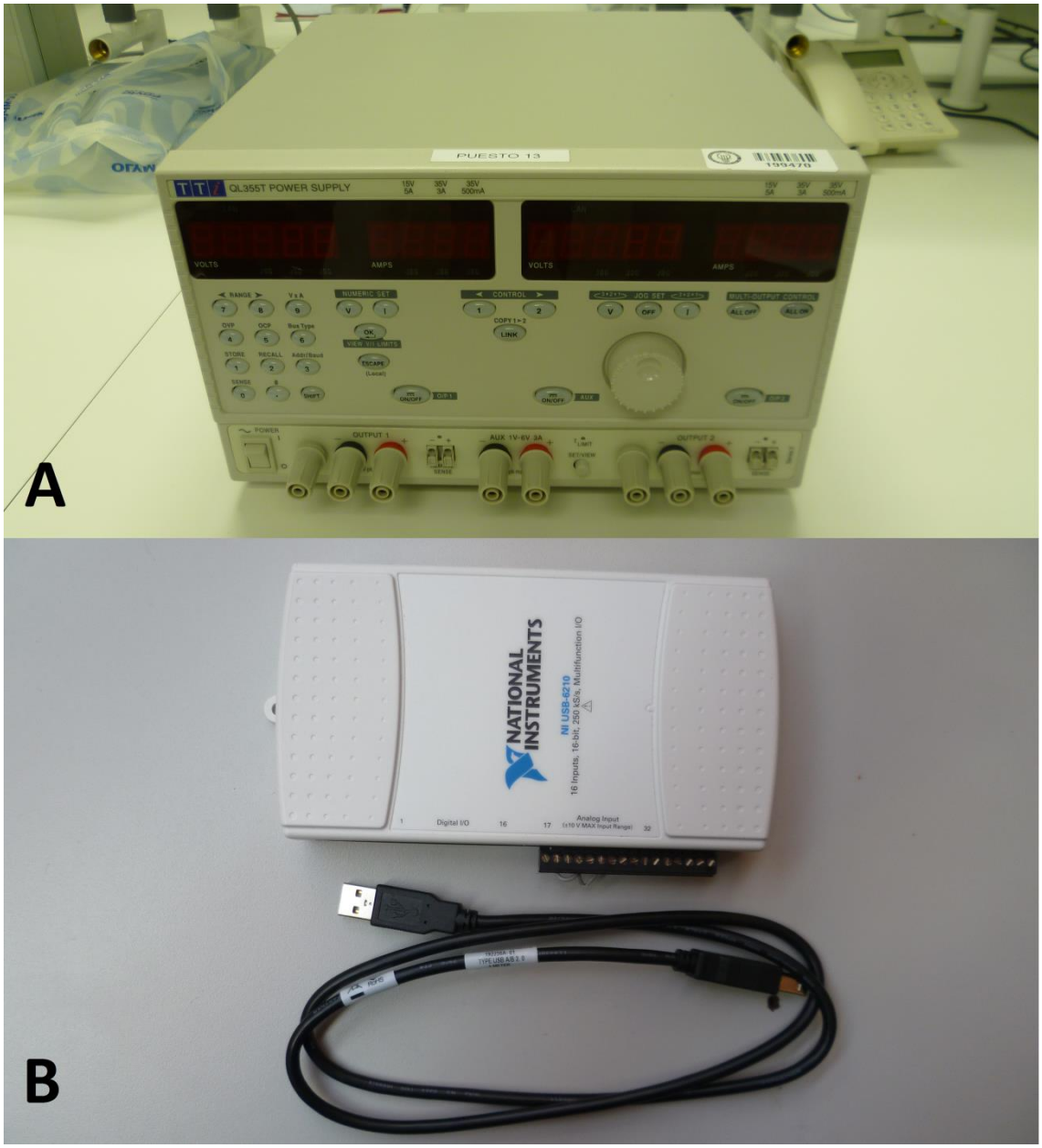

Figure 3.5. Electric devices. (A) Power supply. (B) Micro voltmeter

A microscope (figure 3.6.A) was used to observe the cells, count the available number on each petri dish and check their state. A camera (figure 3.6.B), which is integrated in the microscope, served to take pictures during the experiments.

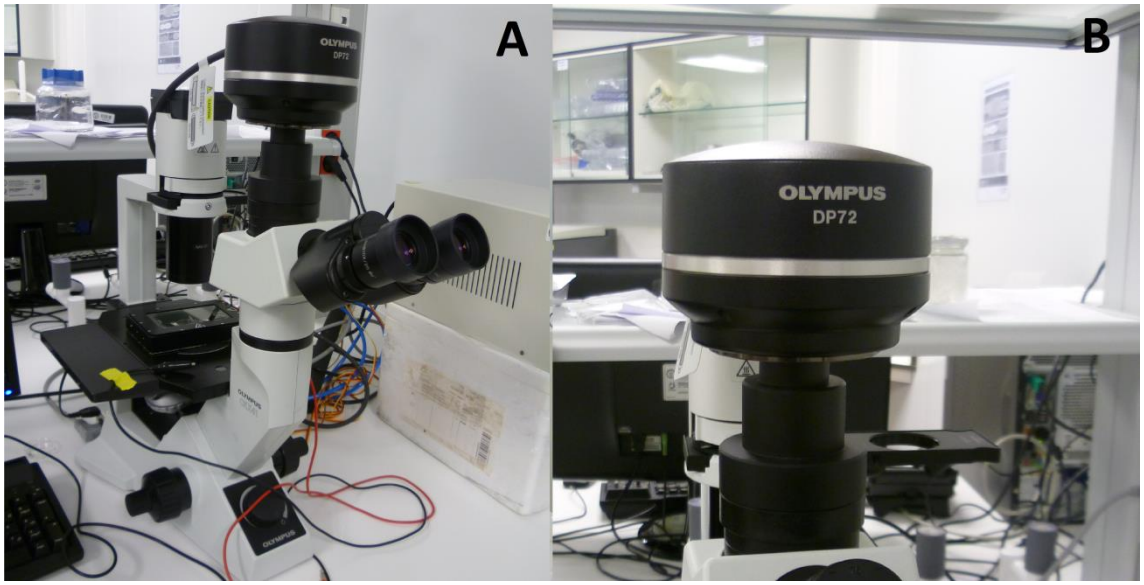

Figure 3.6. Microscope and camera. (A) Micrsocope. (B) Camera.

To acquire and analyze the data, the following programs were used: LabView, ImageJ, Matlab and MouseRecorder.

3.1. CELL CULTURE

Five different procedures were performed to prepare the cells for the experiments. Firstly the medium where the cells will be cultured is prepared. 222.5 mL of DMEM, 25 mL of FBS and 2.5 mL of antibiotic solution are introduced in the vacuum filter. The vacuum filter is connected to the vacuum chamber and all the content descend to the lower chamber, going through the filter. The medium, called DMEM 10 because it has 10% of FBS, is kept in the fridge, at 4 ºC.

Initially, the cells were frozen at - 80 ºC, so it was necessary to unfreeze them. This process needs to be performed fast to reduce the impact on the cells and avoid cellular death. The cryotube where the cells were frozen is introduced in a 37.0 ºC bath. A 15 mL centrifuge tube is prepared with 3 mL of DMEM 10. Once the content of the cryotube becomes liquid, it is added to the previously prepared 15 mL centrifuge tube. The 15 mL centrifuge tube is centrifuged at 1000 r.p.m. for 7 minutes to separate the cells from the freezing medium. The medium is discarded and the pellet is resuspended in 6 mL of DMEM 10 and placed in a p100. The p100 is introduced in the incubator at 37.0 ºC and let cells grow to obtain the amount necessary for the experiments.

The p35 that will be used for the scratch assay should be coated with collagen. 2 mL of a collagen and PBS solution (20 µg of collagen per 50 mL of solution) is poured in a p35. It is let to cure 2 hours under UV light. 1 mL of PBS is used to clean and, then, discarded. The p35 with collagen is left in the fridge until it is needed.

The next procedure consisted on preparing the culture for the experiments. The medium is removed from the p100 and 3 ml of PBS are put in to clean. The PBS is removed and 1 mL of trypsine, previously warmed at 37.0 ºC is added to detach the cells. The p100 is introduced in the incubator at 37.0 ºC for 15 minutes so the trypsine can make its effect. Then, 4 mL of DMEM 10 are added to inactivate trypsine and everything is taken in and out of the pipette several times to dissolve cell clots so all the cells are freely suspended. 10 µL of the cell suspension are introduced in a Neubauer chamber to count the available cells. The rest is transferred to a 15 mL centrifuge tube and centrifuged 7 minutes at 1000 r.p.m. While the centrifuge is working, the number of available cells is calculated: the cells in each 1 mm^2 square are counted and the mean is calculated; to obtain the total number of cells, the mean is multiplied by 10000 and by 5 (the volume in ml where the cells are suspended). After centrifugation, the medium is discarded and DMEM 10 is added. The pellet is resuspended in a volume of DMEM 10 such that the proportion of cells is 1 million per milliliter. The solution is taken in and out of the pipette repeatedly again to avoid cell clusters. 2 mL are introduced in a p35, previously prepared with collagen, which will be used to do the experiment. The rest is put in a new p100, adding DMEM 10 to obtain a final volume of 10 mL. This p100 will be used later to start the process again without the need of defrosting cells. Both petri dishes are introduced in the incubator at 37.0 ºC.

After one day in the incubator, the cells have already grown and attached to the petri dish surface. The p35 is observed under the microscope to check the state of the cells. A pipette tip (the one used for 100 µL to 1 mL, the biggest one) is used to make a straight scratch following the diameter of the petri dish. The medium is discarded and 1 mL of PBS is used to clean. The PBS is removed and 2 mL of DMEM 10 are added. The lid of the p35 is changed by the one containing the wires structure. The wires are placed in the scratch following different distributions depending on the experiment: two on the middle and one on each side of the wound for potential measurement; and two in the middle and two on one of the sides of the wound for potential induction. The p35 is introduced inside the small incubator and stuck so the wires cannot move. The zone of interest is placed under the microscope for further observation of cells behavior.

3.2. ELECTRIC DEVICES

For the potential induction experiment, there was no need of programming or device preparation. The power supply was set to a concrete value, the wires were connected and it was turned on. The distribution of the wires for these experiments consisted on two wires placed in the middle of the wound, where there are no cells, and the other two on top of the cells found on one side of the wound (figure 3.7).

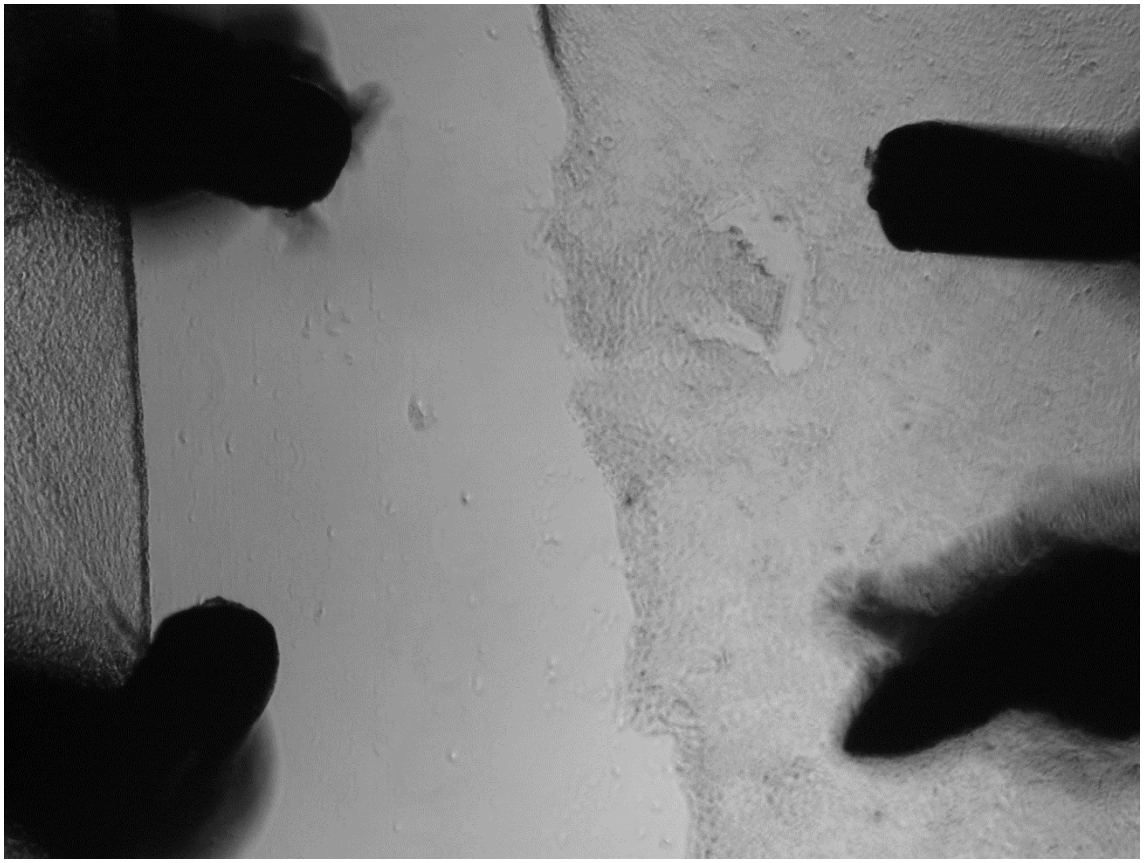

Figure 3.7. Distribution of the wires during induction experiments: two wires in the middle of the wound and the other two on top of the cells on one of the sides.

On the other hand, for the potential measurement, the device had to be programmed. A LabView program was designed to acquire the data and print it in a text file. The program needed as user inputs four parameters: frequency and number of samples taken per measurement, time between measurements and number of measurements. All these parameters were set to the same value for all the experiments (except for the total number of measurements taken during each experiment, which is specified in the results section): frequency and number of samples per measurement, set both to 100 so it acquired 100 samples during 1 second and take the mean as the measurement to filter noise; and time between one measurement and the next one, which was 59 seconds, so time difference between measurements was 1 minute (1 second of acquisition plus 59 waiting). Eight inputs of the device were used to obtain measurements. Those eight inputs were interpreted as four different channels, being four of them the positive

reference for each channel and the other four the negative reference. The configuration of the inputs was changed several times as new experiments were performed. The specific design for each experiment is described in results section. Mainly two different ways of configuration were used: comparative and common. In the comparative form, for each channel, one of the references came from one of the wires placed in the petri dish and the other reference came from a different wire. In the common form, all channels had the same negative reference, which could be an external ground or one of the wires from the petri dish. Within this case, two wires were placed in the middle of the wound and the other two wires on top of the cells on the sides of the wound, one on each side (figure 3.8). As it can be observed, this distribution interfered a lot with the pictures. Later, it will be explained the way this problem affected the experiments and how it was solved.

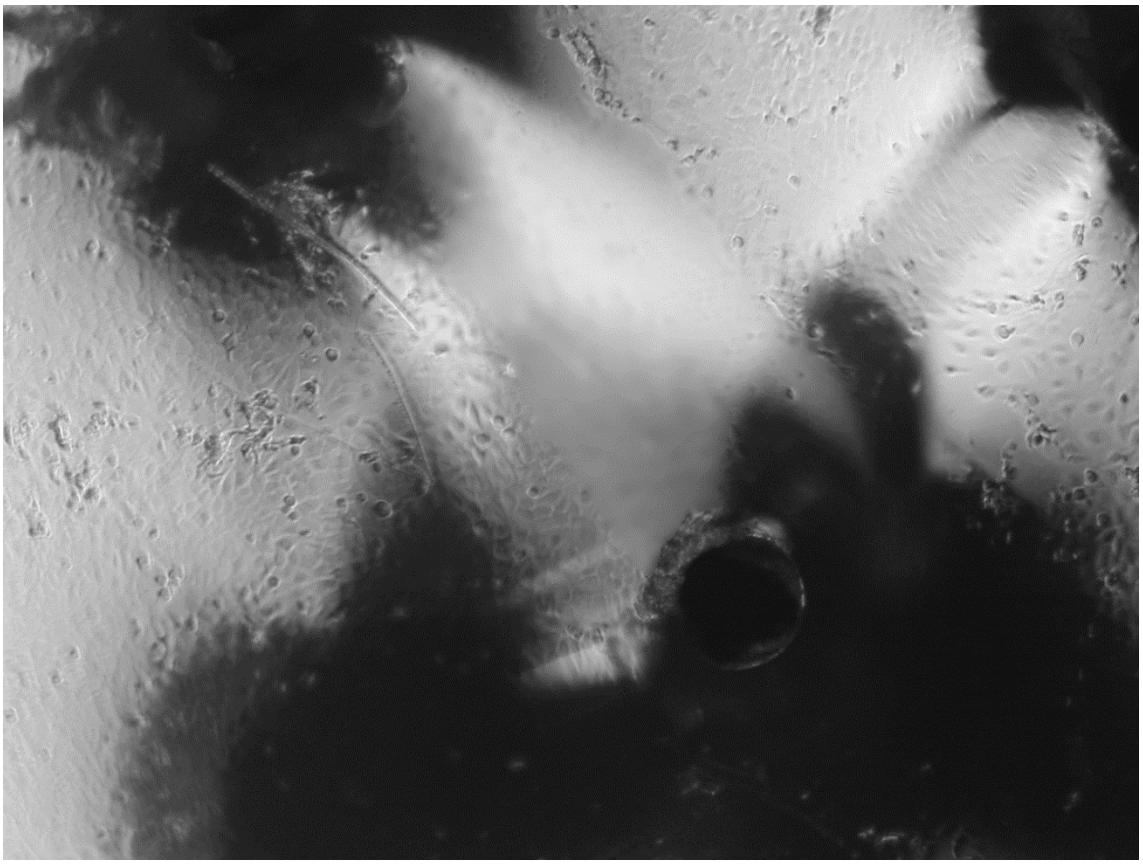

Figure 3.8. Distribution of the wires during potential measuring experiments: two wires in the middle of the wound and the other two on top of the cells on the sides of the wound, one on each side.

3.3. TIME-LAPSE MICROSCOPY

As it was explained on the previous point, the electric device preparation to analyze the behavior during potential induction was quite simple. The objective was to measure the velocity of the cell front. After wires were properly placed and the electric device connected, the petri dish was observed under the microscope. Initially some pictures were taken at 4x, so distance between wires could be calculated for later calibration

(this process is explained on next section, computational analysis). Depending on the exact position of the wires, they might fit on a single picture (figure 3.7) or several images could be needed to calculate the distance between wires (figure 3.9.A, B, C and D). Then, the microscope objective was changed to 10x and focused on the wound border right in the middle of the wires (3.9.E).

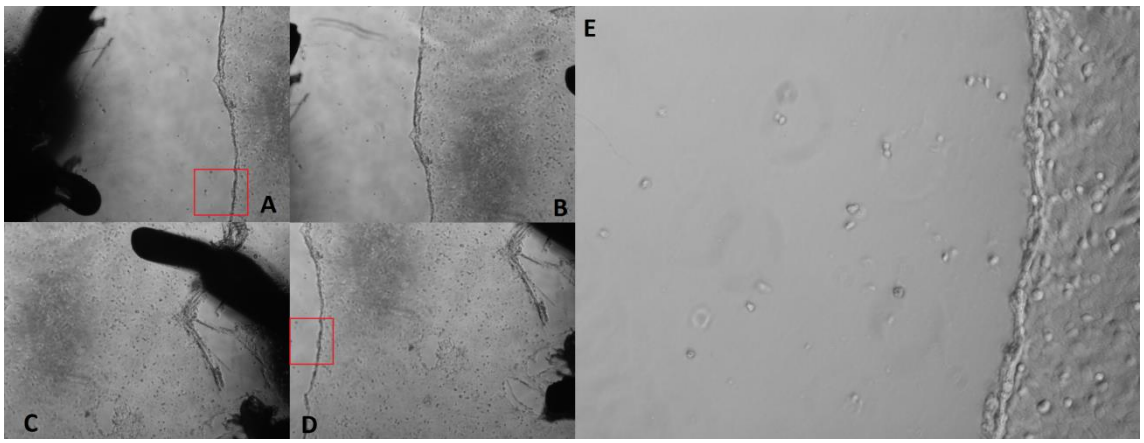

Figure 3.9. 4x pictures (A, B, C and D) and 10x picture (E). The area squared up in (A) and (D) corresponds to the area seen in (E). (A) Distance between the wires inside the wound and the wound border. (B) Distance between the top wires, one from inside the wound and the other on top of the cells. (C) Distance between the wires on top of the cells. (D) Distance between the lower wire on top of the cells and the wound border. (E) Position where the pictures will be taken during the experiment to follow up the wound border movement.

The image acquisition was performed using a macro in ImageJ. The macro used a plugin called Twain6 to take a picture with the camera and save it in a specified folder. Each time a new picture was saved, the name assigned to that picture contained a number that were consecutive for all the pictures. A txt file is created to store the date each turn a picture was acquired, which will be later used to calculate the time difference between pictures and the velocity.

Finally, the process of taking pictures was automated. The experiments last several hours and one picture should be taken each 2 - 3 minutes so it was not possible to have one person doing it manually. A program called MouseRecorder was used. The program is able to save specific mouse paths and clicks. The acquisition procedure was saved and the parameters for time between images and number of images were set. Then, the device was left several hours taking pictures of the wound border where the potential was applied.

3.4. COMPUTATIONAL ANALYSIS

After the measuring experiments, the data was saved on a txt file. The file was loaded in Matlab as a matrix containing the measurements from one channel in each column. The information was then plotted to analyze it. Due to the difficulty on acquiring high quality pictures from potential measuring (the distribution interfered a lot with the field

of view), the wire distribution around the wound for each experiment was recorded as a schematic image (figure 3.10). The distance between wires would be also very difficult to calculate using these pictures, so it was previously set to be approximately 1.5 mm between wire 3 and the rest of the wires; thus, the distance between wire 1 and wires 2 and 4 would be around 2.12 mm; and distance between wires 2 and 4 would be 3 mm.

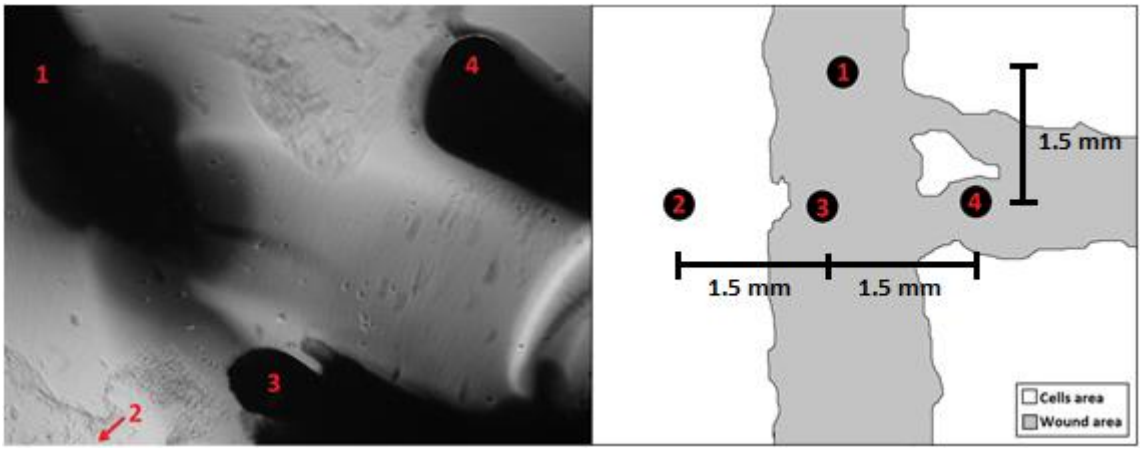

Figure 3.10. Example of schematic wire distribution. Picture with an example on wire distribution (left) and the corresponding schema (right).

For the potential induction, the data analysis required more resources due to the image processing needed. First of all, the images were calibrated. A picture of the lines of a Neubauer chamber was taken with both 10x and 4x objectives (figure 3.11). The pixel size can be easily calculated because the separation between lines in a Neubauer chamber (0.25 mm) is known. Four points, strategically distributed forming a rectangle (figure 3.11), are selected:

10x picture (figure 3.11.A):
Point 1 (406,358) Point 2 (1166,360) Point 3 (406,742) Point 4 (1166,744)
Rectangle dimensions: 0.5 mm x 0.25 mm

4x picture (figure 3.11.B):
Point 1 (428,434) Point 2 (1042,437) Point 3 (429,894) Point 4 (1042,896)
Rectangle dimensions: 1 mm x 0.75 mm

Based on these data, the pixel size is obtained: 1.63 μm^2/pixel for 4x images and 0.65 μm^2/pixel for 10x images.

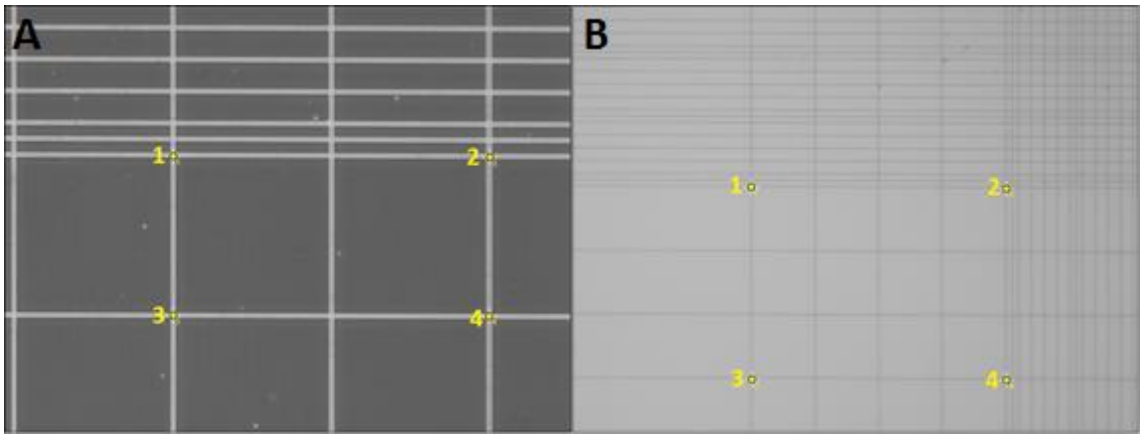

Figure 3.11. Pixel size calculation. (A) 10x picture: 0.65 µm2/pixel. (B) 4x picture: 1.63 µm2/pixel.

Once the real distances are known, the pictures were analyzed. Initially, a qualitative analysis of the displacement was performed. The images were observed as a video and the position of the cells' edge and cell density along the whole set of images was compared. Then, a quantitative analysis of the cells' border velocity was carried out. This quantitative analysis was composed of several steps. An initial filtering was necessary due to several artifacts, mainly because of the shade coming from the wires, but also small scratches produced during wire positioning and the cells distribution itself. The filter needed to be adjusted for every experiment, but the usual procedure was background subtraction and contrast enhancement (figure 3.12), which is a common way to eliminate illumination artifacts. The filtering step was performed with ImageJ: once the specific procedure for a concrete experiment was decided, a macro was built to repeat it along all the images from that experiment.

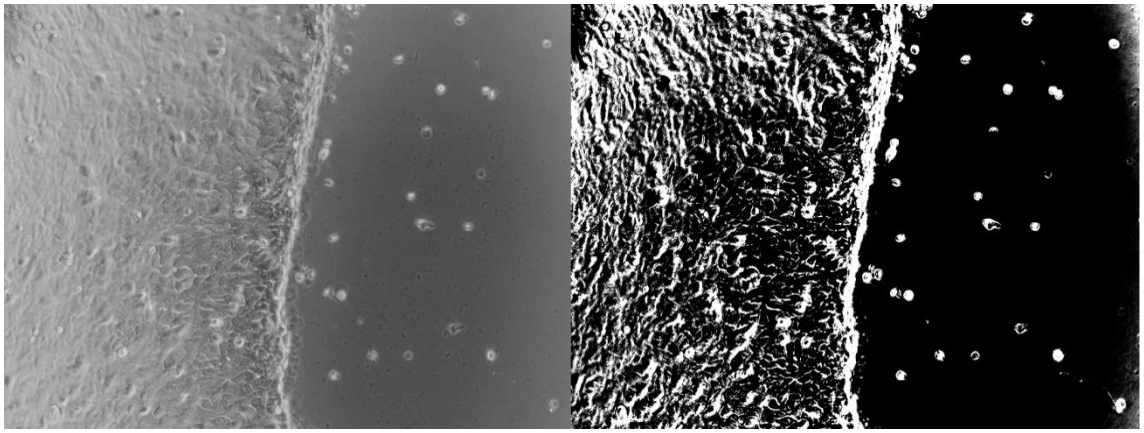

Figure 3.12. Image filtering. Original image (left) and the same image after filtering (right).

After the images are filtered, further analysis was performed with Matlab. The images were loaded one by one and the position of the border was searched, so the movement of cells towards (or away from) the wound could be measured. The algorithm started asking the user for the folder where the images were stored and the number of images to be analyzed. The first image is shown and the user selects three points of the border, one

on the top part, another one in the central zone and the last one on the lower part of the image. These three points are used to make an initial approximation of the border (figure 3.13.A). A smaller matrix is built around the area selected and the position of the border will be searched within this matrix. For the rest of the images, the matrix is built around the border from the previous image (figure 3.13.B). Once the position of the border has been localized for all the images, the velocity is calculated dividing the distance between the border in one image and the border in the next one by the time between images acquisition.

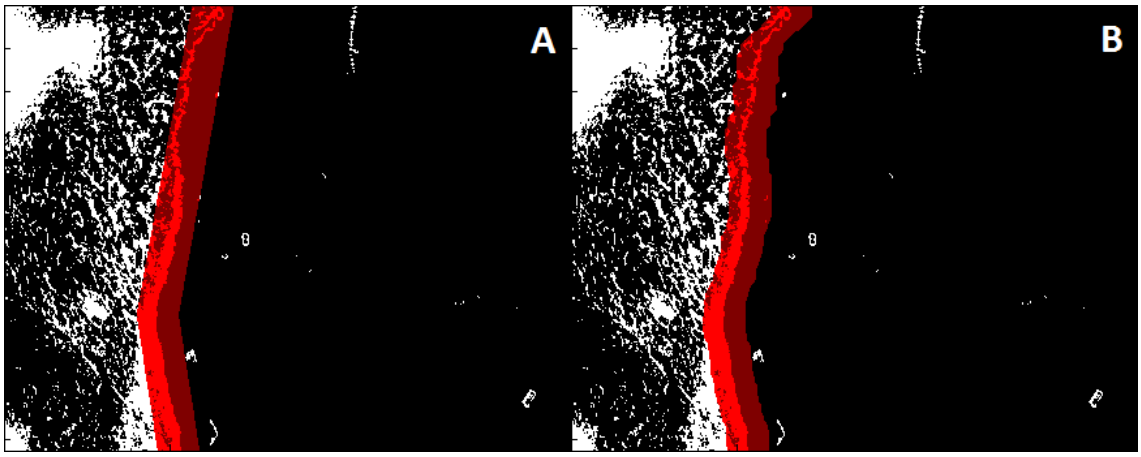

Figure 3.13. Example on border searching: the algorithm reduces the searching area only to a zone close to the known position of the border (in red). (A) Initial searching area, looking for user selection. (B) Searching area after some images have been analyzed: border adaptation.

4. RESULTS

4.1. POTENTIAL MEASUREMENT

** Note: the graphics show the potential measured during the experiments, to obtain the electric field associated, the values have to be multiplied by the correspondent distance.*

EXPERIMENT 1

Time: 24 hours

Common configuration
Channel A: + wire 1; - incubator's metal housing
Channel B: + wire 2; - incubator's metal housing
Channel C: + wire 3; - incubator's metal housing
Channel D: + wire 4; - incubator's metal housing

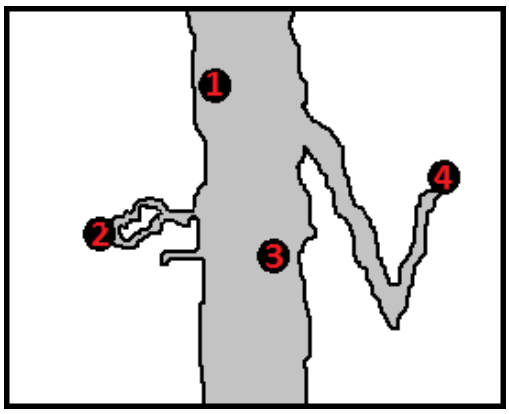

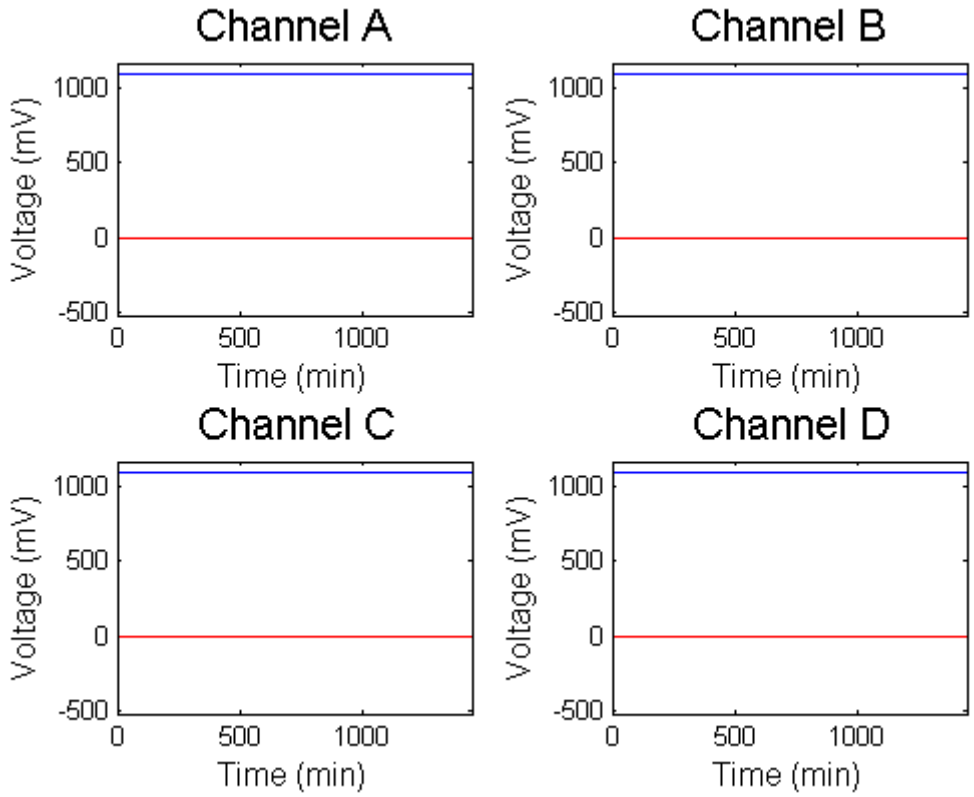

Figure 4.1. Wire distribution and graphics with the measured potentials for experiment 1.

Observations:
All the measurements are saturated to the maximum value that the micro voltmeter accepts. The incubator's metal housing is not a good reference as ground.

EXPERIMENT 2

Time: 24 hours

Common configuration
Channel A: + wire 1; - plug ground
Channel B: + wire 2; - plug ground
Channel C: + wire 3; - plug ground
Channel D: + wire 4; - plug ground

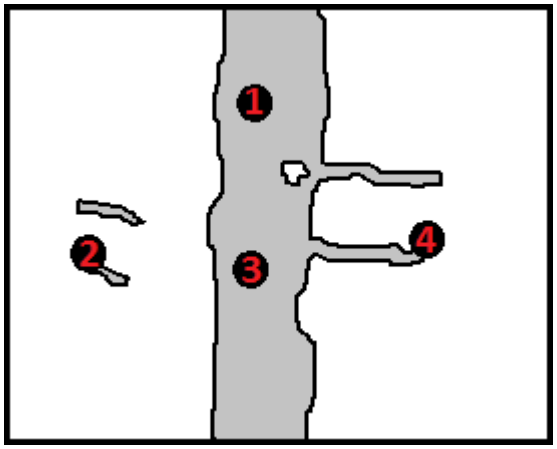

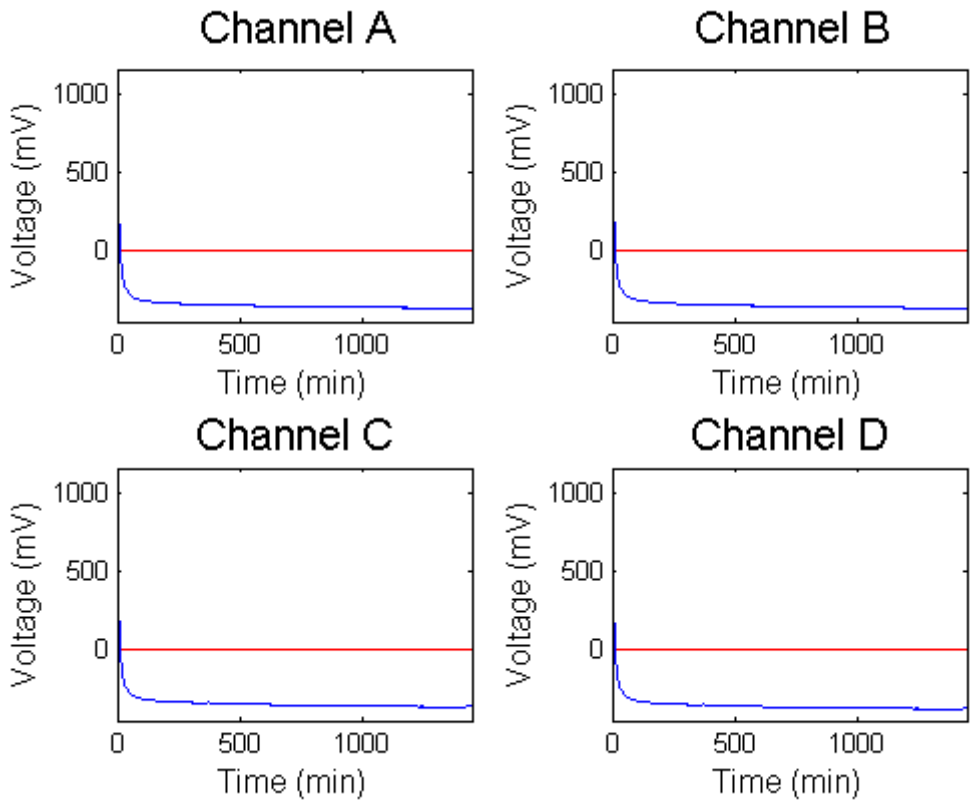

Figure 4.2. Wire distribution and graphics with the measured potentials for experiment 2.

Observations:
The four channels seemed to measure the same and tend to a value very different from the expected one (to be consistent with the bibliography, the values would need to be on a range around 10 to 100 mV [11]). The plug ground is not a good reference.

EXPERIMENT 3

Time: 24 hours

Common configuration
Channel A: + wire 2; - wire 3
Channel B: + wire 1; - wire 3
Channel C: + wire 4; - wire 3
Channel D: unused

** Note: low cell density*

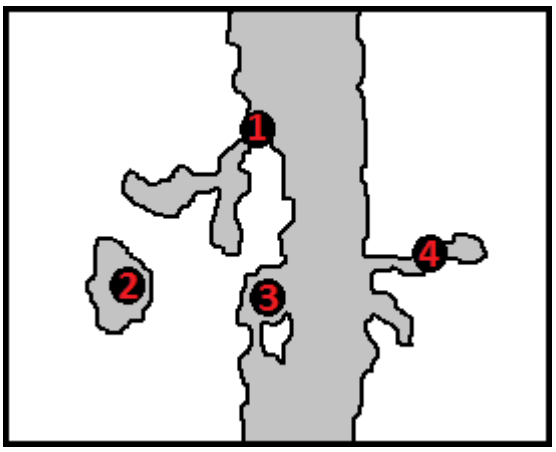

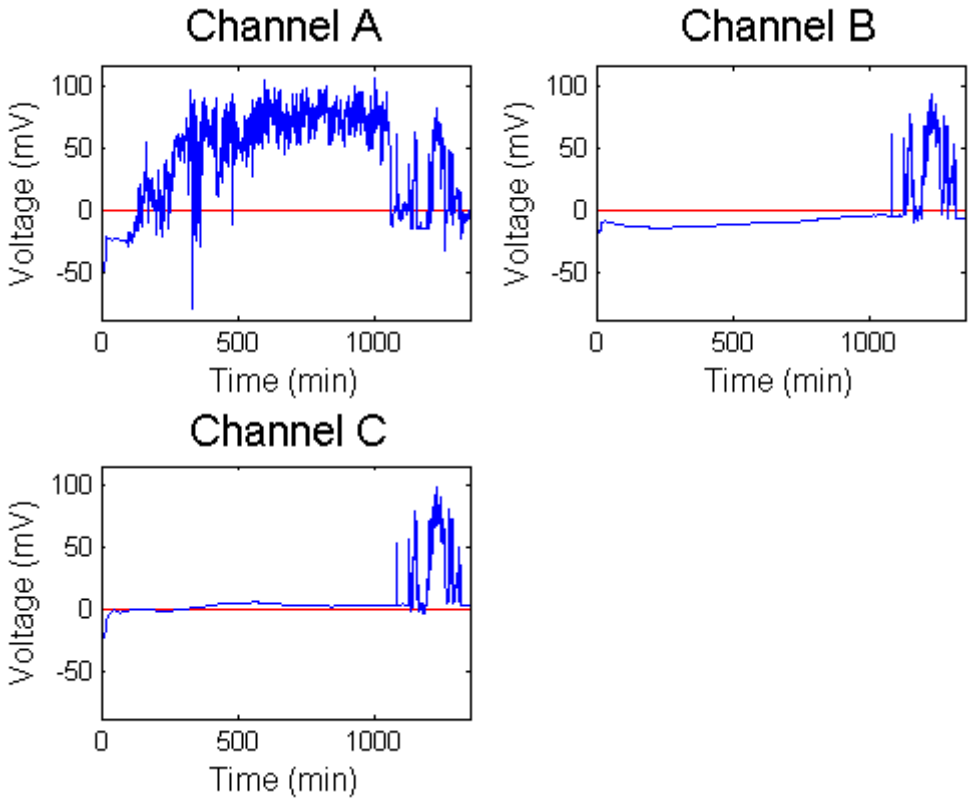

Figure 4.3. Wire distribution and graphics with the measured potentials for experiment 3.

Observations:
The graphics do not show any coherent behavior (a guess for the strange measurements could be that it is due to the low cell density), but they fit on the expected voltage range. It seems that the best idea is to use one of the wires as the reference.

EXPERIMENT 4

Time: 15 hours

Common configuration
Channel A: + wire 2; - wire 3
Channel B: + wire 1; - wire 3
Channel C: + wire 4; - wire 3
Channel D: unused

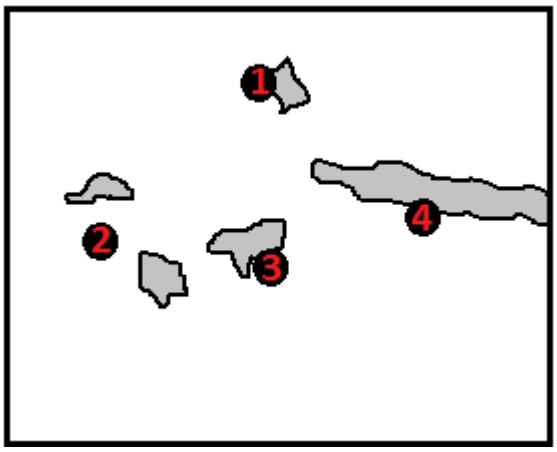

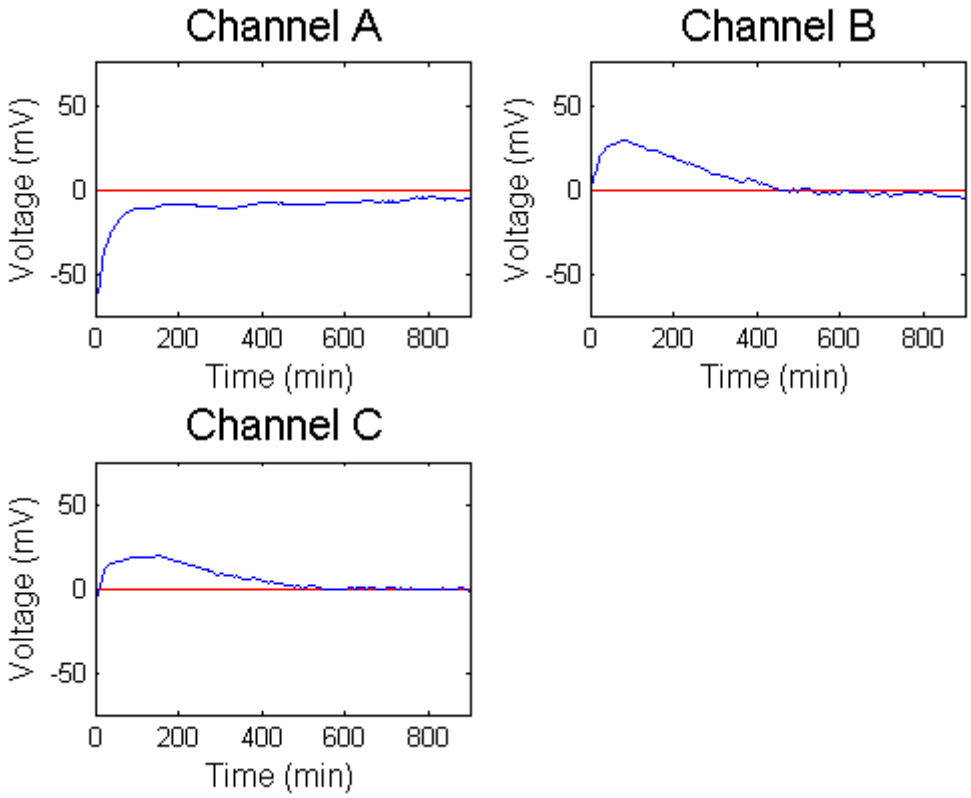

Figure 4.4. Wire distribution and graphics with the measured potentials for experiment 4.

Observations:
No scratch performed, aiming to observe whether a potential is measured while no wound is present.
All channels tend to 0. The initial peaks could be due to the small scratches produced during wire positioning.

EXPERIMENT 5

Time: 20 hours

Common configuration
Channel A: + wire 2; - wire 1
Channel B: + wire 3; - wire 1
Channel C: + wire 4; - wire 1
Channel D: unused

** Note: very high cell density*

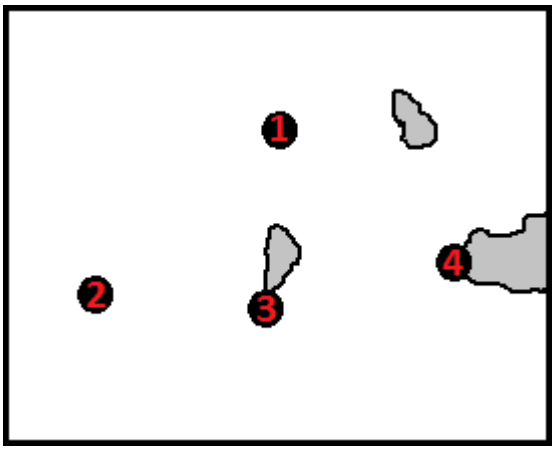

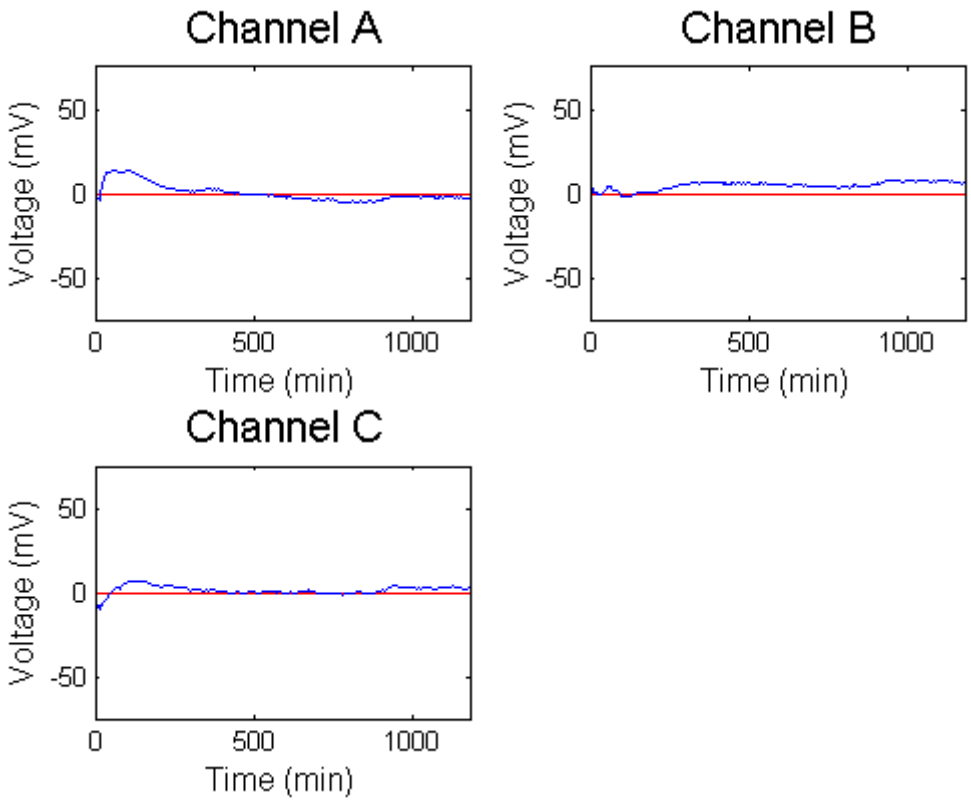

Figure 4.5. Wire distribution and graphics with the measured potentials for experiment 5.

Observations:
All channels keep close to 0 along the whole time they are measured, which is the expected behavior as there was no scratch and, thus, no wound.

EXPERIMENT 6

Time: 25 hours

Differential configuration
Channel A: + wire 1; - wire 2
Channel B: + wire 3; - wire 4
Channel C: + wire 2; - wire 3
Channel D: + wire 4; - wire 3

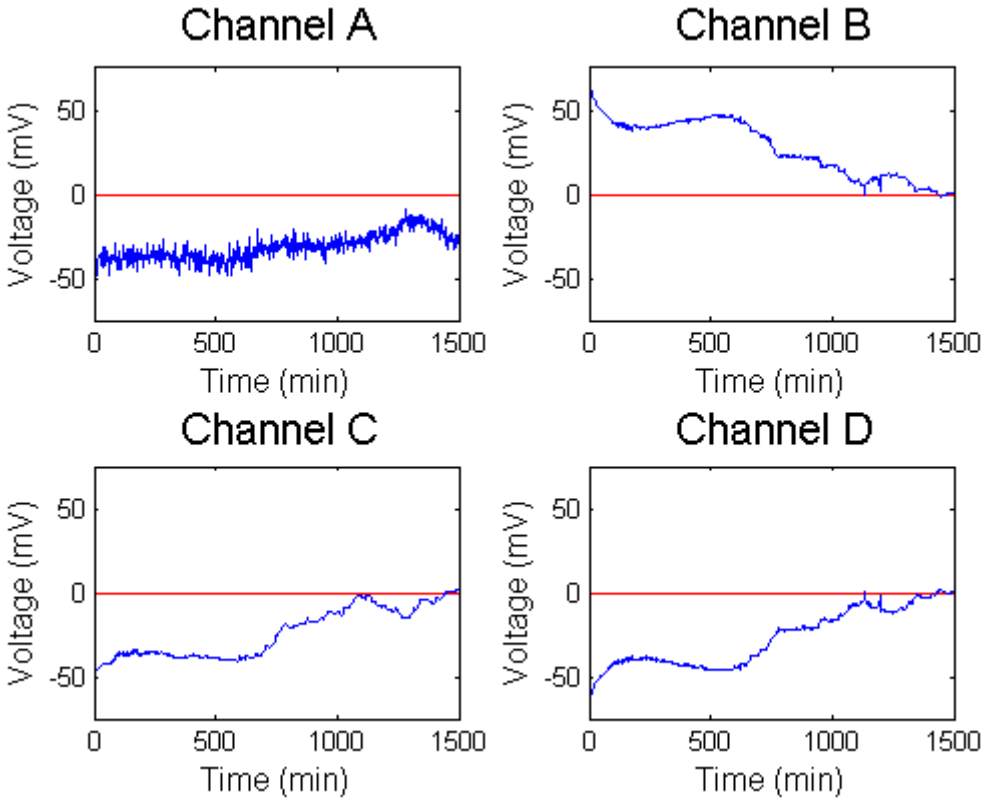

Figure 4.6. Wire distribution and graphics with the measured potentials for experiment 6.

Observations:
Channels B and D are measuring the same with opposite sign; their sum must be 0 for consistency of the measurements (figure 4.7).
Channels A and C reflect the difference between the center of the wound in two different points and the left side. As the center of the wound is supposed to have positive potential compared to the side, measurements from channel A should be positive and measurements from channel C negative.

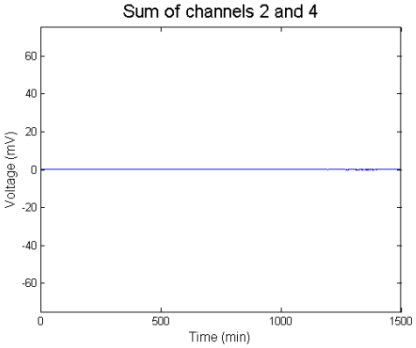

Figure 4.7. Sum of channels B and C from experiment 6.

EXPERIMENT 7

Time: 48 hours

Differential configuration
Channel A: + wire 1; - wire 3
Channel B: + wire 3; - wire 2
Channel C: + wire 2; - wire 4
Channel D: + wire 4; - wire 3

** Note: very low cell density*

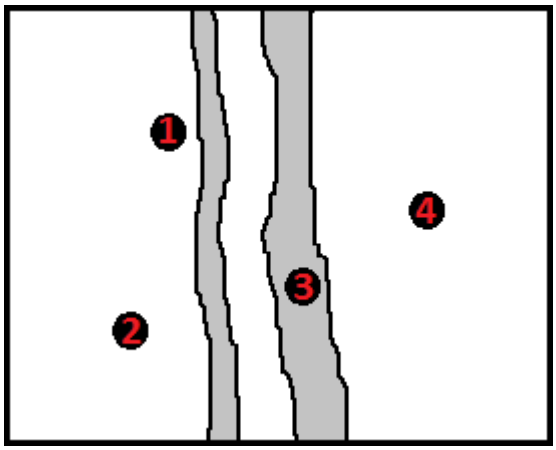

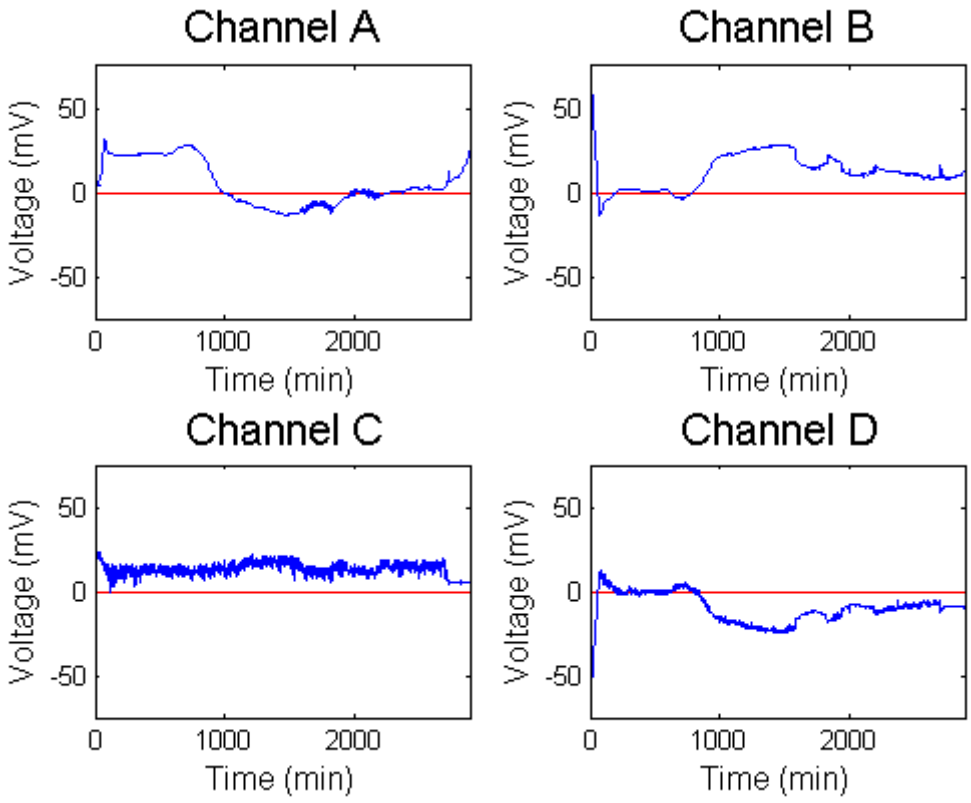

Figure 4.8. Wire distribution and graphics with the measured potentials for experiment 7.

Observations:
Channel C measures the potential difference between both sides, fairly constant.
Channels B and D measure the difference between the middle and both sides of the wound. Initially, it tends to 0, probably due to low cell density. They, then, rise to show a difference around 20 - 25 mV, with higher potential in the middle of the wound, and this difference slowly starts to descend.
Channel A shows a behavior similar to channel D, which make sense because it compares, the potential on one side to the potential in the middle. The inexpliwire problem is an approximately 20 mV offset. A possible reason could be the diagonal position respect to the wound.

EXPERIMENT 8

Time: 20 hours

Differential configuration
Channel A: + wire 2; - wire 1
Channel B: + wire 3; - wire 2
Channel C: + wire 1; - wire 4
Channel D: + wire 4; - wire 3

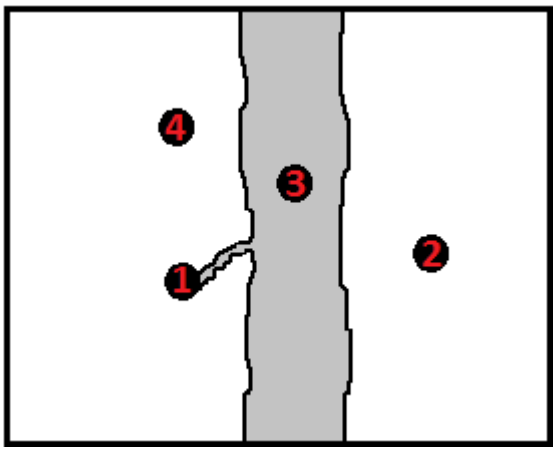

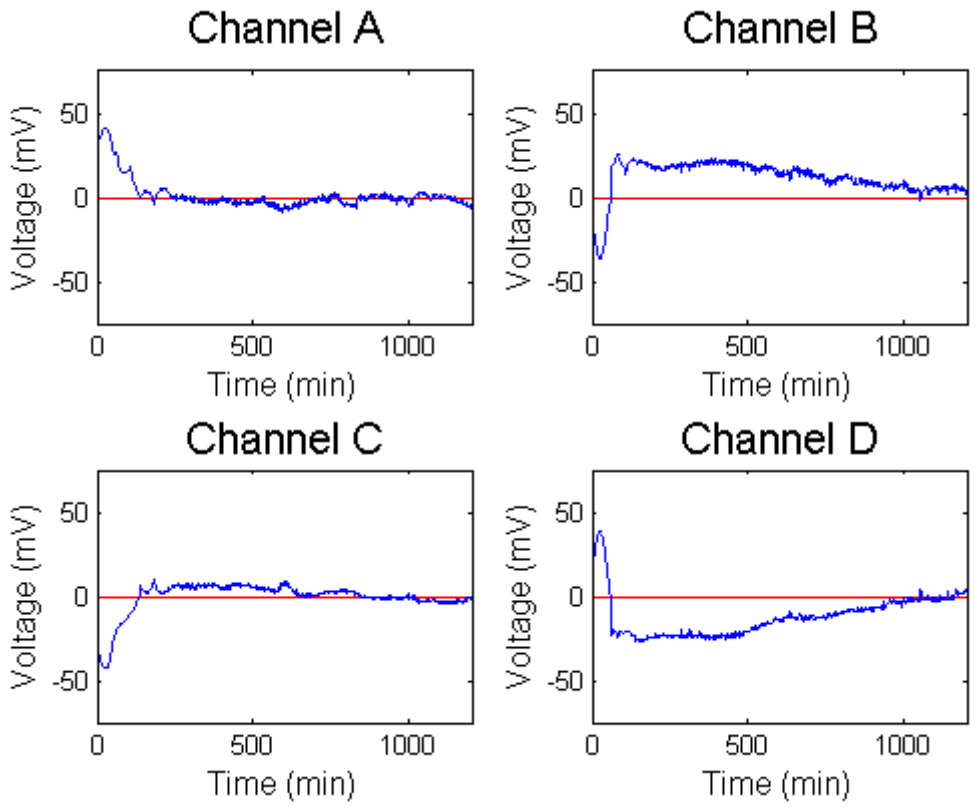

Figure 4.9. Wire distribution and graphics with the measured potentials for experiment 8.

Observations:
Channels A and C are related to the difference between both sides of the wound and between two points on the same side, respectively. Both have an initial peak, probably due to the small scratch next to wire 1, but, after this peak, they keep quite close to 0.
Channels B and D show the difference between the middle of the wound and the sides. They have an initial reverse peak, which might have its explanation on the cells behavior right after the scratch, when they firstly go a little bit backwards before the wound starts closing. Then, they reach a value of around 25 mV difference between the middle and the side (in channel B the positive reference is the center, while in channel D the positive reference is the side), and slowly descend to 0.

EXPERIMENT 9

Time: 25 hours

Differential configuration
Channel A: + wire 1; - wire 3
Channel B: + wire 2; - wire 3
Channel C: + wire 4; - wire 2
Channel D: + wire 3; - wire 4

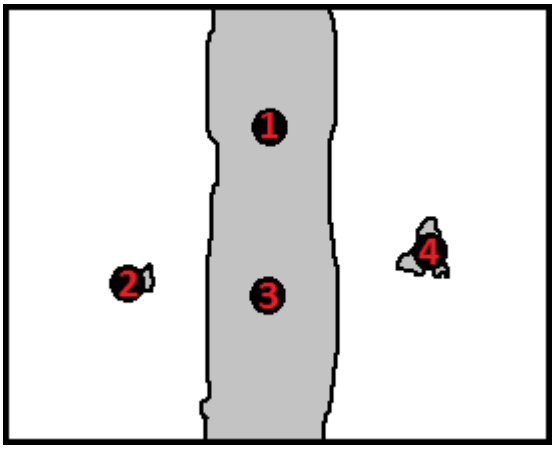

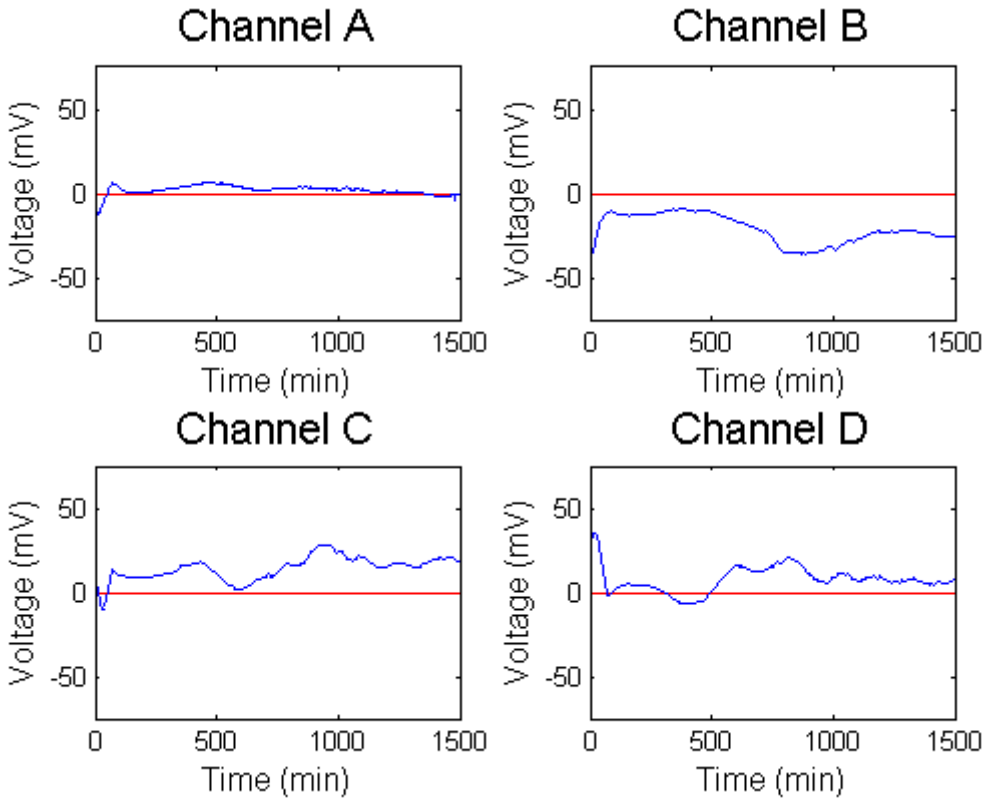

Figure 4.10. Wire distribution and graphics with the measured potentials for experiment 9.

Observations:
Channel A shows potential difference for two points inside the wound and is close to 0. Channel C is related to the difference between both sides. It is probably affected by the small scratches produced while positioning wires B and D. It is positive, which would agree with the fact that the scratch around wire 4 (+ reference in channel C) is bigger. Channels B and D compare the potential between the center of the wound and the sides. They show that the potential in the middle is higher. The difference seems to increase after several hours, which could be due to the close of the small wounds formed around wires 2 and 4. Channel D is closer to 0, probably because the scratch surrounding wire 4 is wider.

EXPERIMENT 10

Time: 25 hours

Differential configuration
Channel A: + wire 4; - wire 3
Channel B: + wire 3; - wire 1
Channel C: + wire 2; - wire 4
Channel D: + wire 3; - wire 2

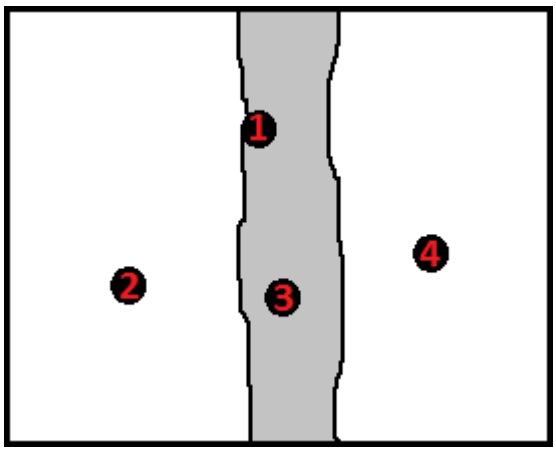

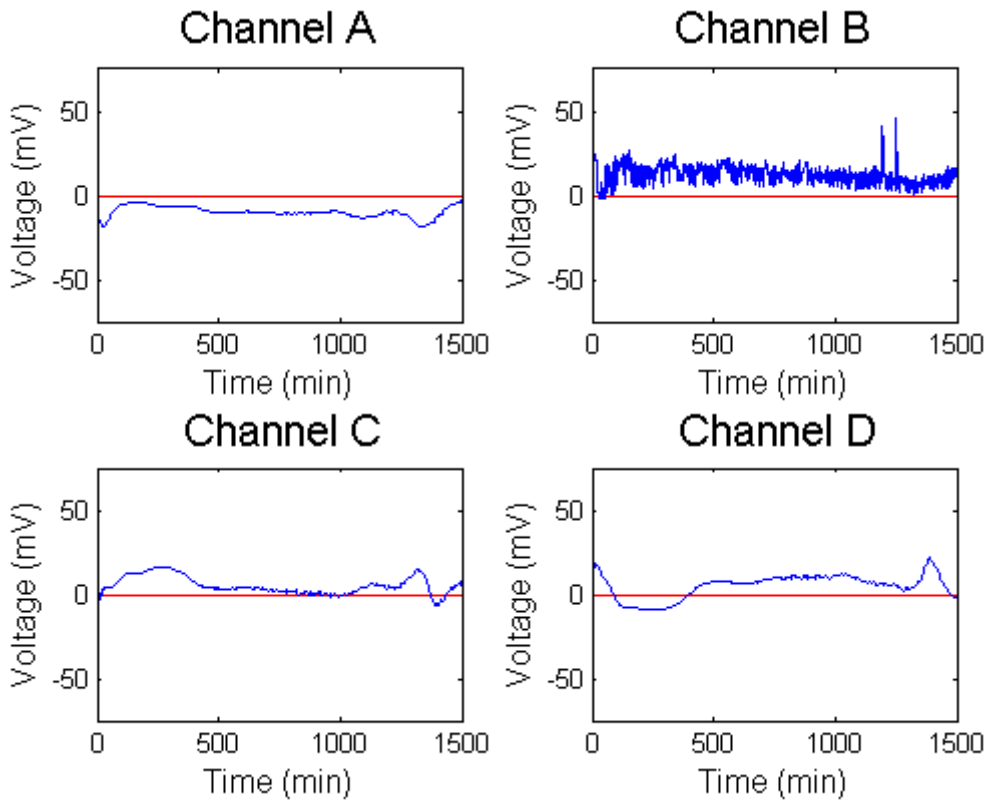

Figure 4.11. Wire distribution and graphics with the measured potentials for experiment 10.

Observations:
The noise in channel B might be due to the cells pushing wire 1 during their development towards wound center (a displacement between original and final position was observed on wire 1).
Channel C compares both sides of the wound, it seems to tend to 0 after a while, but in the end, it has two peaks that have no explanation.
Channels A and D measure the difference between the center of the wound and the sides. It can be observed that, generally, the center has higher potential. The difference is small, which might be explained by the fact that small scratches are produced when positioning wires 2 and 4.

EXPERIMENT 11

Time: 24 hours

Common configuration
Channel A: + wire 1; - wire 4
Channel B: + wire 3; - wire 4
Channel C: + wire 2; - wire 4
Channel D: unused

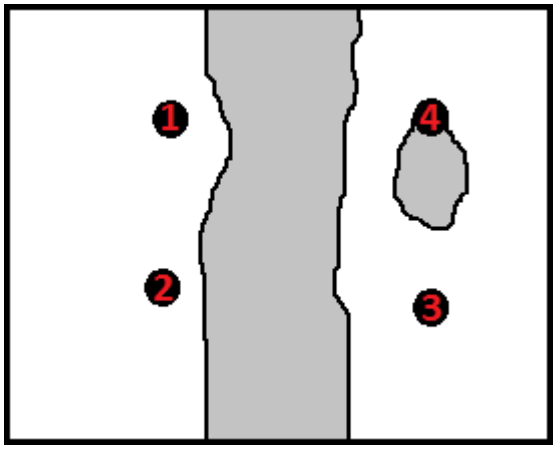

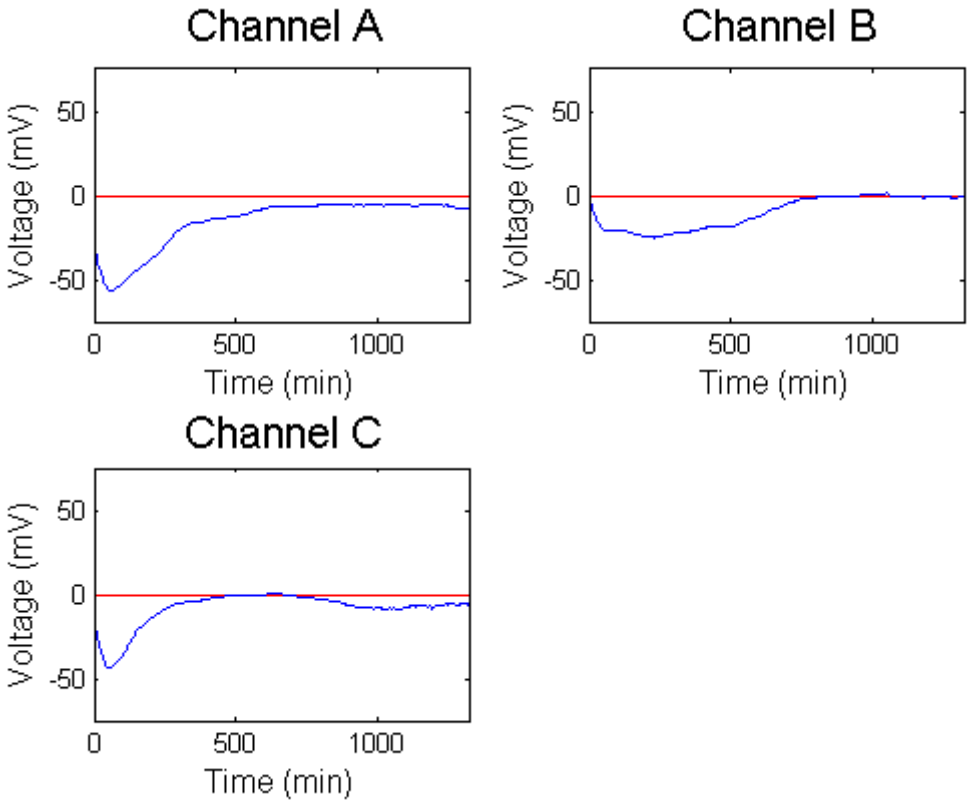

Figure 4.12. Wire distribution and graphics with the measured potentials for experiment 11.

Observations:
Wire distribution was changed to observe the potential from a different point of view.
Channel B shows the difference on the same side of the wound. It has an initial difference, probably due to the scratch around wire 4. Interpreting this small scratch as a wound, the potential inside the scratch would be higher. Anyway, the difference goes to 0 after some time.
Channels A and C are related to the difference between both sides. They initially have a high peak, but also go close to 0 (not as much as channel B, but they are on the other side of the wound, so they might have more interferences).

EXPERIMENT 12

Time: 17.5 hours

Common configuration
Channel A: + wire 4; - wire 1
Channel B: + wire 4; - wire 3
Channel C: + wire 4; - wire 2
Channel D: unused

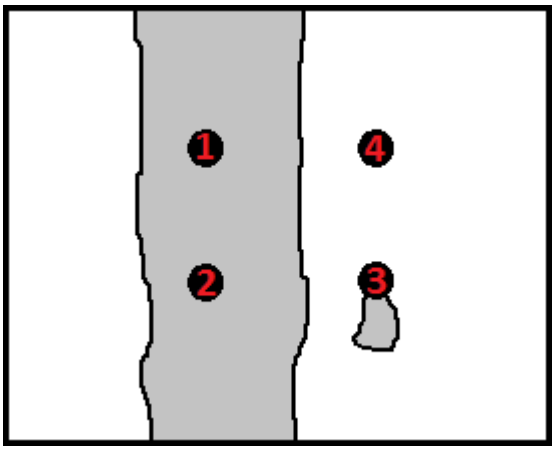

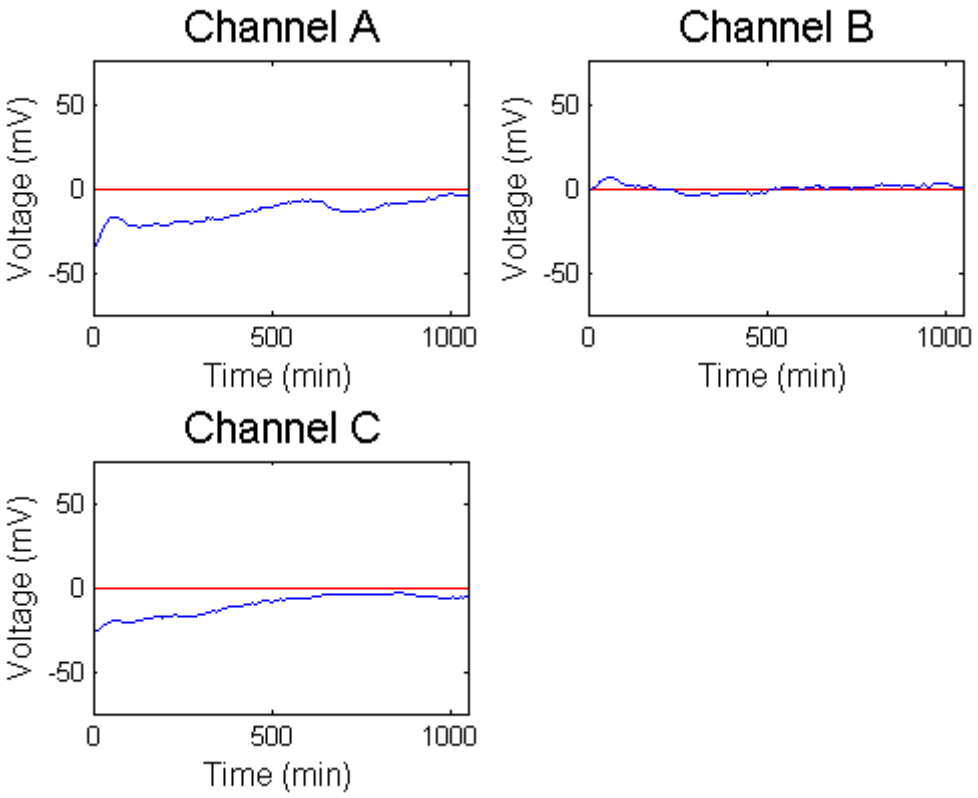

Figure 4.13. Wire distribution and graphics with the measured potentials for experiment 12.

Observations:
Channel B stays close to 0 because it is measuring the difference between the two wires on top of the cells.
Channels A and C show the difference between the side and the middle of the wound. It can be observed that the center of the wound has higher potential and the difference descends as time passes and wound closes.

4.2. POTENTIAL INDUCTION

EXPERIMENT 13

Voltage: 0 V; No wires, control experiment.
Total number of images: 568
Time between images: 178 s; **Total time:** 28 hours

Qualitative analysis:
Initially, the cells' border goes a little bit away from the center of the wound, then it starts going towards the middle of the wound at quite constant speed.
Cell density stays quite constant on time and space. Cells reproduce, so the net number increases, but their migration towards the wound maintains cell density. Also the density is similar between the zone close to the wound and further zones.

Quantitative analysis (450 pictures analyzed)**:**

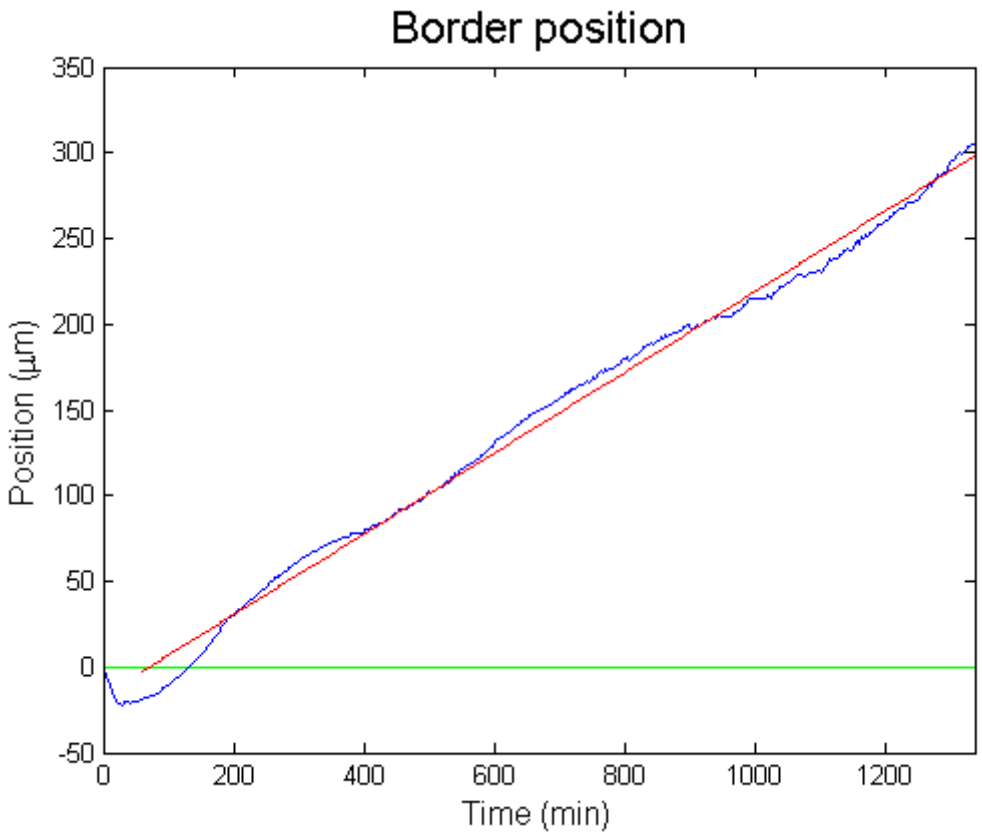

Figure 4.14. Evolution of the cells' border (blue) and linear approximation (red) for experiment 13.

p = 0.2355t - 16.6108

Velocity (from t=60) = 0.235 µm/min.

** Note: the sign of the experiments has been selected as positive (+) when the potential is higher in the center of the wound and negative (-) when the potential is smaller in the center of the wound. It has been determined this way to follow the observed behavior on the measuring experiments.*

EXPERIMENT 14

Voltage: +50 mV; **Electric field:** 30 mV/mm
Total number of images: 440
Time between images: 172 s; **Total time:** 21 hours

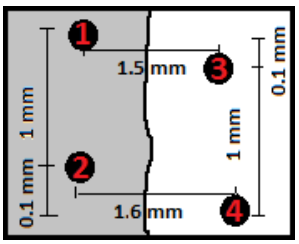

Figure 4.15. Wire distribution in experiment 14.

Qualitative analysis:
In this case a recessive phase is not observed, cells directly start moving towards the center of the wound.
Cell density seems to be constant on time and space.

Quantitative analysis (2 pictures analyzed)**:**
The illumination artifacts did not allow processing images one by one to obtain the edge position (figure 4.16). A general approximation was performed supposing closely constant velocity: the position in the initial image was compared to the position in the final image (figure 4.16).

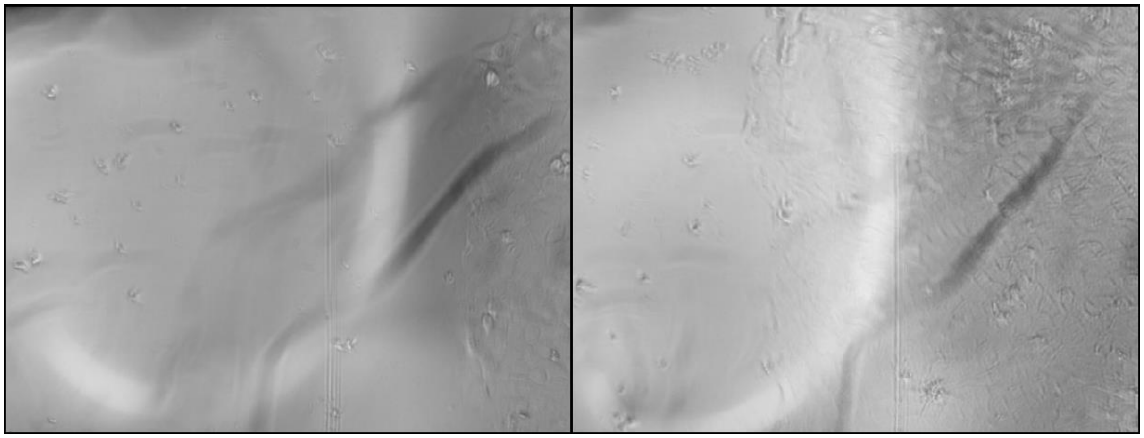

Figure 4.16. Evolution of the cells' border for experiment 14.

Distance between initial and final position of the border: 423.8 µm
Time between initial and last images: 1260 min.

Velocity (approximated to constant the whole time) = 0.336 µm/min.

EXPERIMENT 15

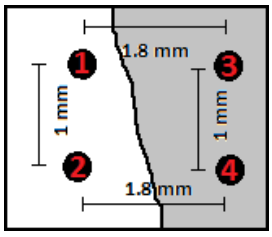

Figure 4.17. Wire distribution in experiment 15.

Voltage: +100 mV; **Electric field:** 55 mV/mm
Total number of images: 405
Time between images: 169 s; **Total time:** 19 hours

Qualitative analysis:
The cell edge goes a little bit away from the wound center at the beginning and, then, the cells move towards wound center at fairly constant velocity.
Cell density seems to stay constant in time and space.

Quantitative analysis (295 pictures analyzed)**:**

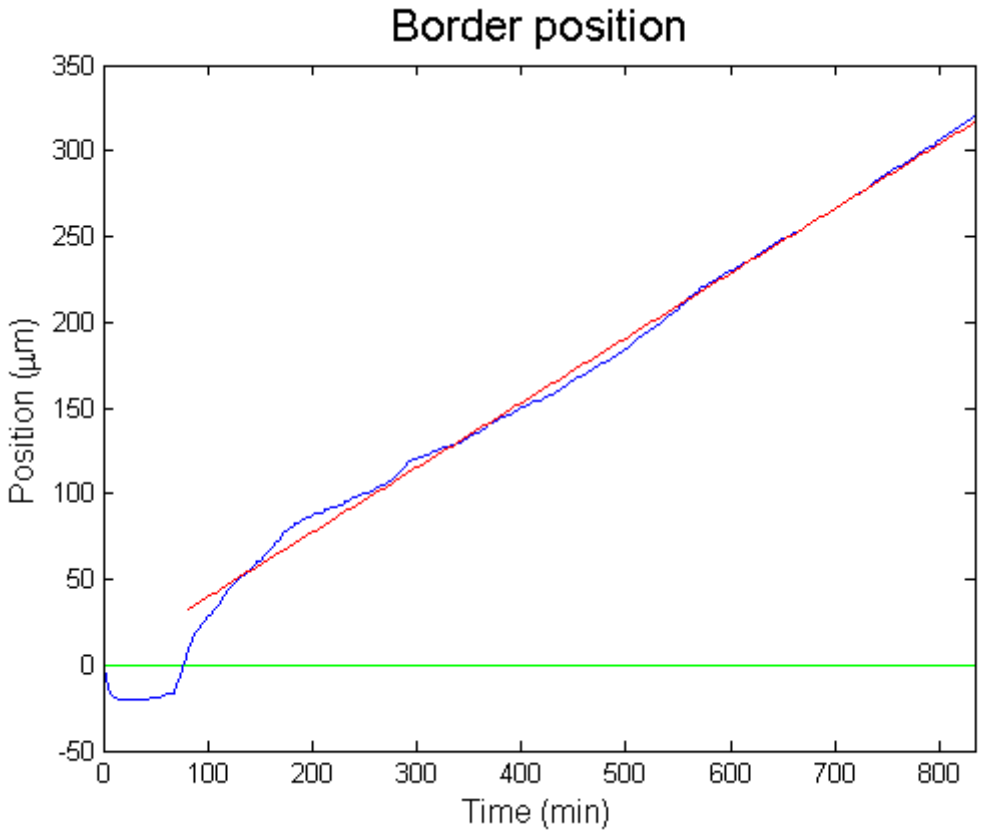

Figure 4.18. Evolution of the cells' border (blue) and linear approximation (red) for experiment 15.

$p = 0.3777t + 1.7897$

Velocity (from t=80) = 0.378 µm/min.

EXPERIMENT 16

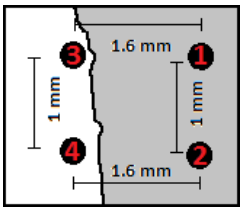

Figure 4.19. Wire distribution in experiment 16.

Voltage: +200 mV; **Electric field:** 125 mV/mm
Total number of images: 576
Time between images: 169 s; **Total time:** 27 hours

Qualitative analysis:

The cell edge goes away from the wound center at the beginning for a longer time than expected from previous experiments. Then, the cells move towards wound center at fairly constant velocity.

Cell density seems to stay constant in time and space for a while after the cells start moving to the center. But, later, the cell density in the wound edge seems to decrease, it seems that the cells right in the border go faster than their neighbors, and some of them even detach from the cell mass in their movement towards the wound center.

Quantitative analysis (425 pictures analyzed)**:**

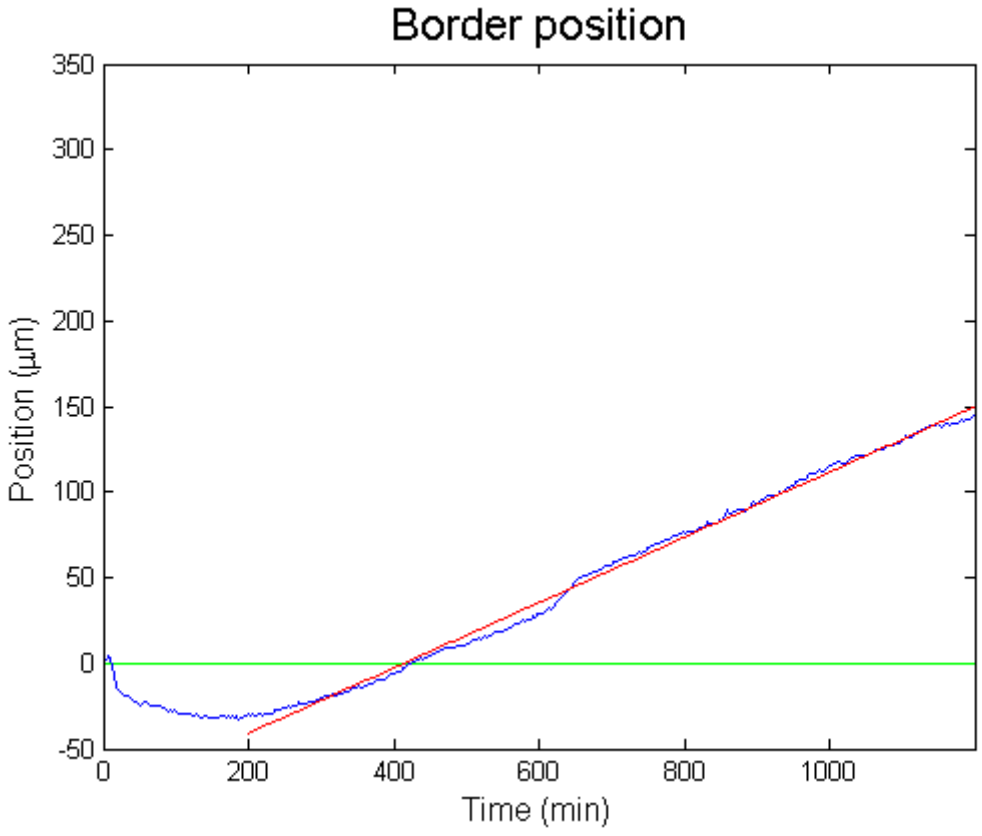

Figure 4.20. Evolution of the cells' border (blue) and linear approximation (red) for experiment 16.

p = 0.1906t - 78.9449

Velocity (from t=200) = 0.19 µm/min.

EXPERIMENT 17

Voltage: +200 mV; **Electric field:** 165 mV/mm
Total number of images: 442
Time between images: 169 s; **Total time:** 20.75 hours

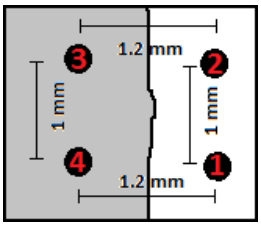

Figure 4.21. Wire distribution in experiment 17.

Qualitative analysis:
The cell edge goes a little bit away from the wound center at the beginning. Then, the cells start moving towards the middle of the wound at constant velocity, after a while, the velocity seems to decrease and it keeps at this slower rate until the end.
Cell density seems to stay constant in time and space.

Quantitative analysis (440 pictures analyzed)**:**

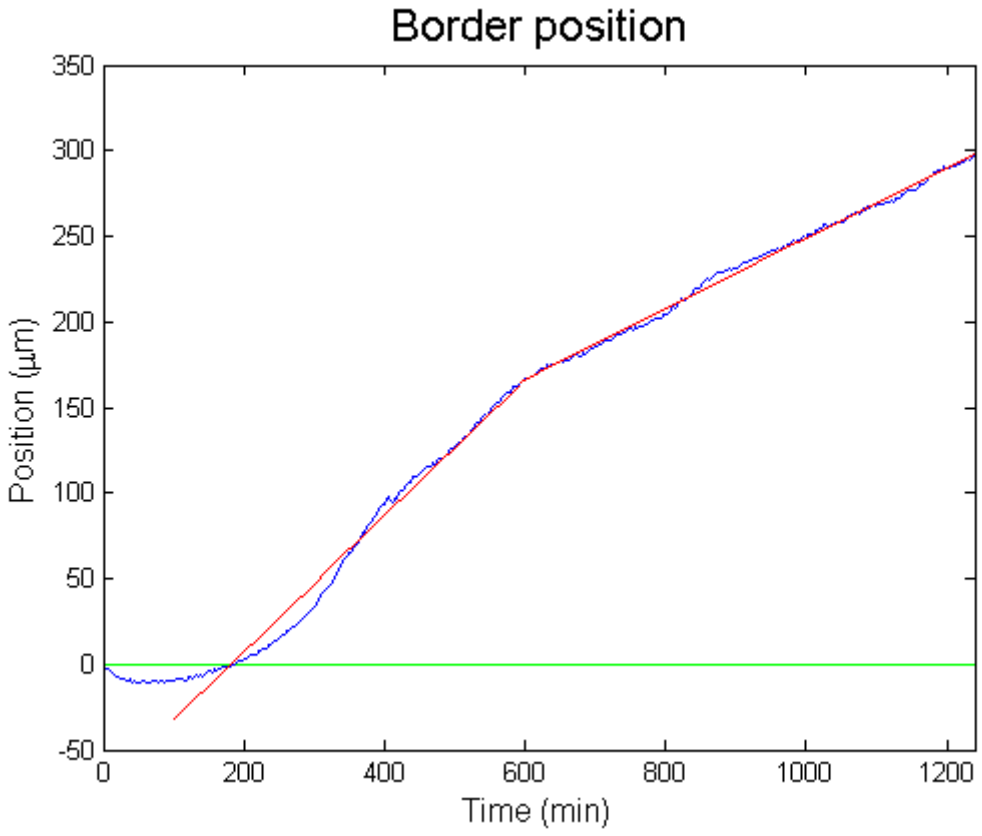

Figure 4.22. Evolution of the cells' border (blue) and two stages linear approximation (red) for experiment 17.

$p_1 = 0.3976t_1 - 72.2019$; $p_2 = 0.2061t_2 + 42.8918$

Velocity (from t=100 to t=590) = 0.398 µm/min.
Velocity (from t=590) = 0.206 µm/min.

EXPERIMENT 18

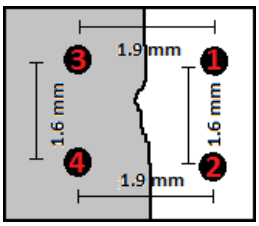

Figure 4.23. Wire distribution in experiment 18.

Voltage: +300 mV; **Electric field:** 155 mV/mm
Total number of images: 479
Time between images: 171 s; **Total time:** 22.75 hours

Qualitative analysis:
The recessive phase is very small and the cells rapidly start moving towards the wound center. They move at constant velocity for a while, then they slow down and keep moving again constantly at this slower rate.
Cell density stays quite constant in time and space.

Quantitative analysis (475 pictures analyzed)**:**

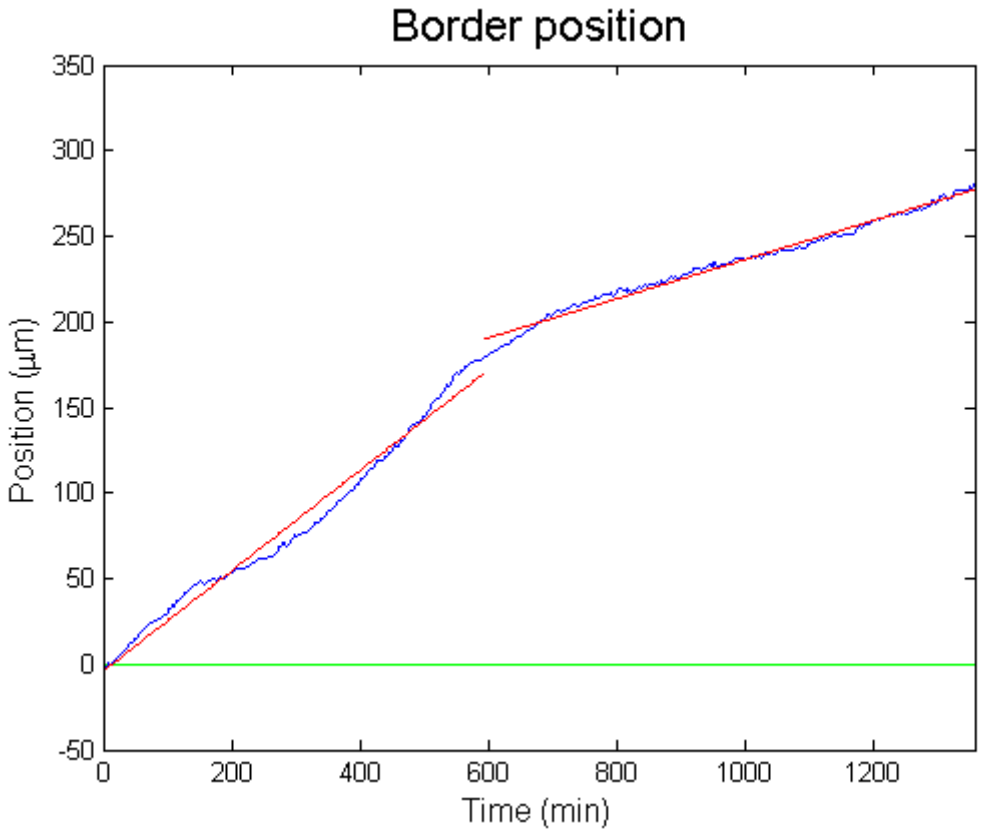

Figure 4.24. Evolution of the cells' border (blue) and two stages linear approximation (red) for experiment 18.

$p_1 = 0.2937t_1 - 4.1216$; $p_2 = 0.1145t_2 + 121.9376$

Velocity (from t=0 to t=590) = 0.294 µm/min.
Velocity (from t=590) = 0.115 µm/min.

EXPERIMENT 19

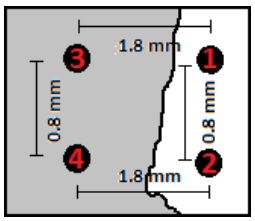

Figure 4.25. Wire distribution in experiment 19.

Voltage: +500 mV; **Electric field:** 275 mV/mm
Total number of images: 402
Time between images: 168 s; **Total time:** 18.75 hours

Qualitative analysis:
Initially, the cells go opposite to the wound center. Then, they initiate to go towards wound center (slower than in any previous experiment), until a moment when they start to go back, opening the wound again. Finally the cell border stabilizes and do not move. Cell density stays quite constant in space. In time, cell density increases, as cells keep reproducing even wound is not closing.

Quantitative analysis (395 pictures analyzed)**:**

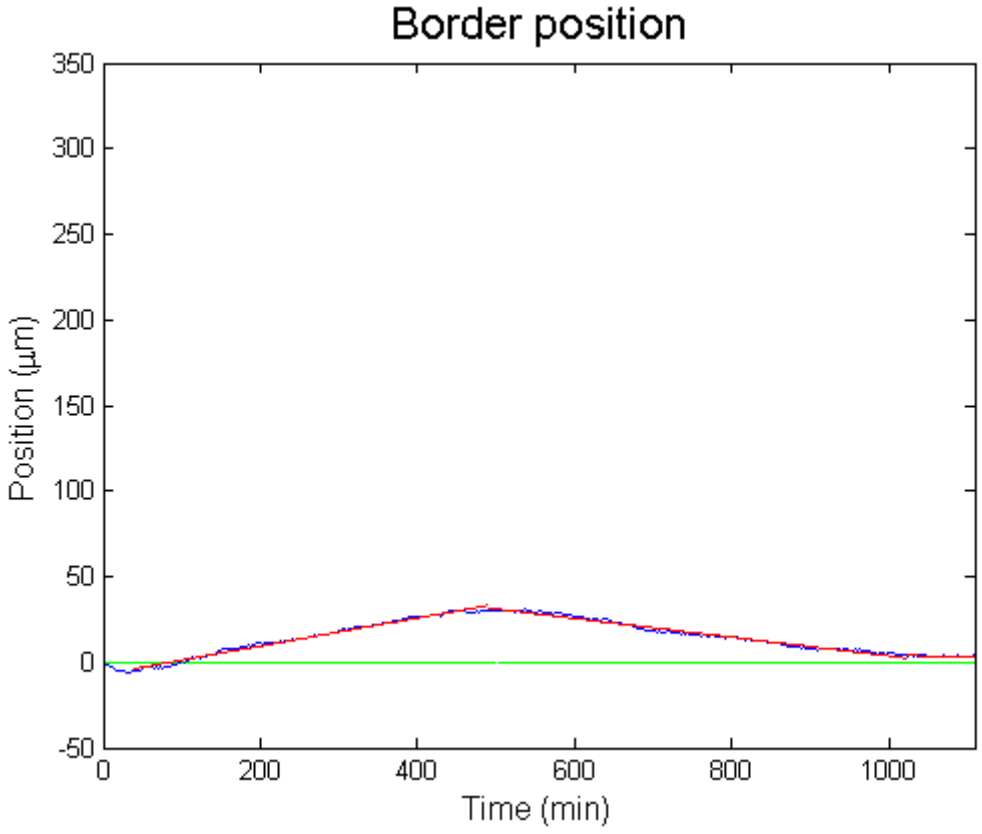

Figure 4.26. Evolution of the cells' border (blue) and two stages linear approximation (red) for experiment 19.

$p_1 = 0.0821t_1 - 6.9789$; $p_2 = -0.0549t_2 + 58.4847$

Velocity (from t=40 to t=490) = 0.082 µm/min.
Velocity (from t=490) = - 0.055 µm/min.

EXPERIMENT 20

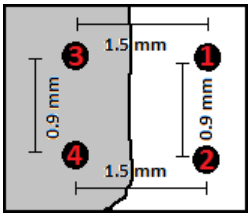

Figure 4.27. Wire distribution in experiment 20.

Voltage: +700 mV; **Electric field:** 465 mV/mm
Total number of images: 547
Time between images: 168 s; **Total time:** 25.5 hours

Qualitative analysis:
The cells start moving towards wound center for a small time. Then, they repeat three or four times a strange behavior: going a bit away from wound center and stop for a while. Cell density is fairly constant in space. In time, cell density increases, as cells keep reproducing even wound is not closing.

Quantitative analysis (490 pictures analyzed)**:**

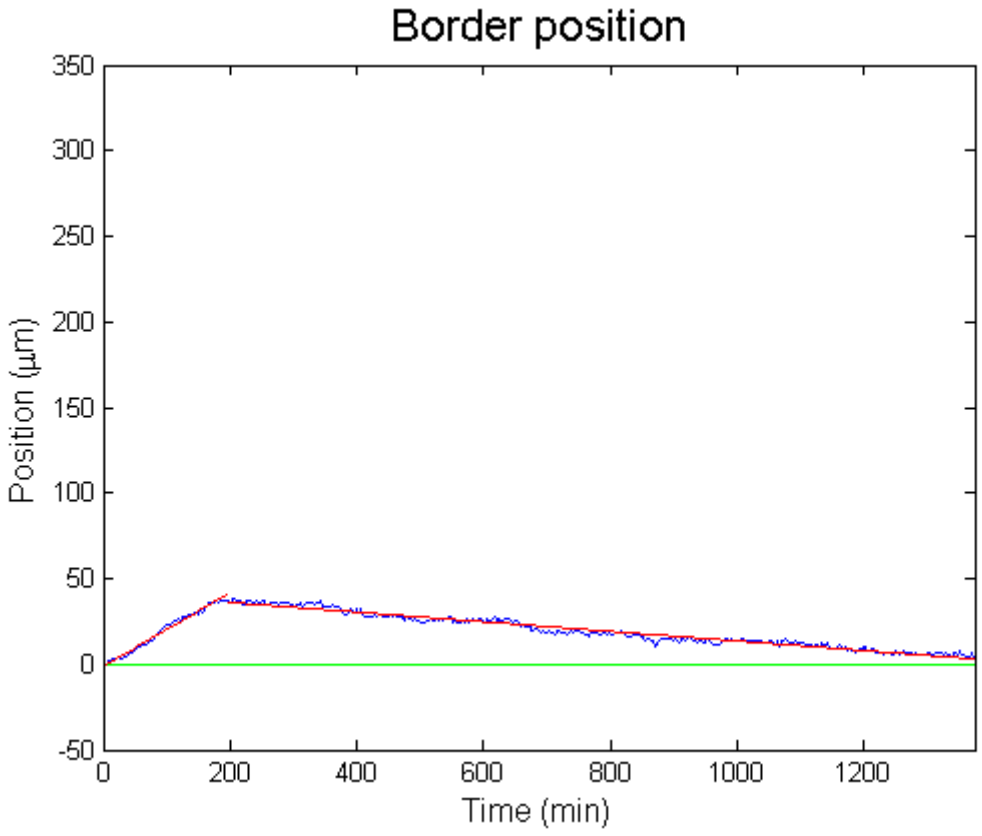

Figure 4.28. Evolution of the cells' border (blue) and two stages linear approximation (red) for experiment 20.

$p_1 = 0.2150t_1 - 1.2465$; $p_2 = -0.0281t_2 + 41.6789$

Velocity (from t=0 to t=195) = 0.215 µm/min.
Velocity (from t=195) = - 0.028 µm/min.

EXPERIMENT 21

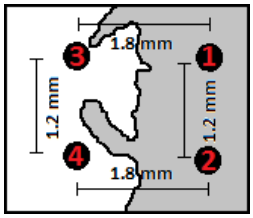

Figure 4.29. Wire distribution in experiment 21.

Voltage: - 300 mV; **Electric field:** - 165 mV/mm
Total number of images: 421
Time between images: 171 s; **Total time:** 20 hours

Qualitative analysis:
Cells move directly towards wound center at a speed that decreases with time, so at the end the movement seems to stop.
Cell density is initially constant in space, but, as time passes, it decreases in the zone closer to the cell edge and increases a lot on further zones.

Quantitative analysis (395 pictures analyzed)**:**

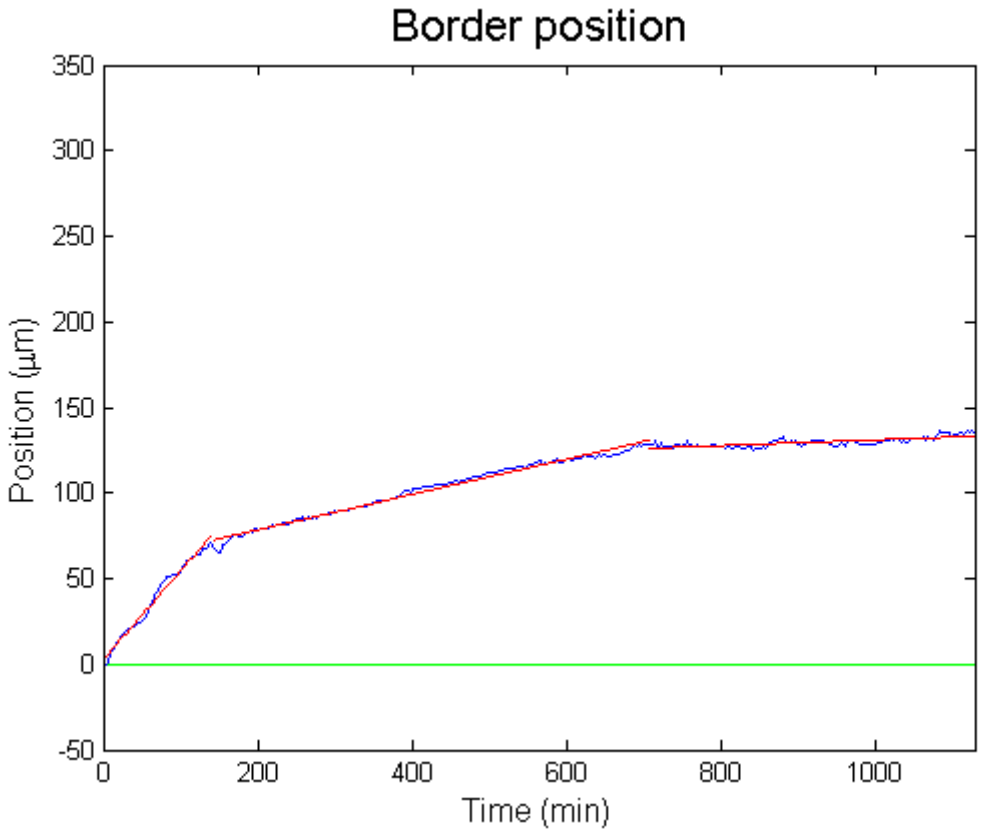

Figure 4.30. Evolution of the cells' border (blue) and three stages linear approximation (red) for experiment 21.

$p_1 = 0.5153t_1 + 2.9767$; $p_2 = 0.1032t_2 + 57.8605$ $p_3 = 0.0170t_3 + 114.0240$

Velocity (from t=0 to t=190) = 0.515 µm/min.
Velocity (from t=190 to t=705) = 0.103 µm/min.
Velocity (from t=705) = 0.017 µm/min.

EXPERIMENT 22

Voltage: - 500 mV; **Electric field:** - 275 mV/mm
Total number of images: 525
Time between images: 168 s; **Total time:** 24.5 hours

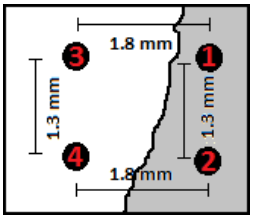

Figure 4.31. Wire distribution in experiment 22.

Qualitative analysis:
Cell border seems not to move for a long time, then, it goes a little bit away from the wound center.
Meanwhile, the cells are not observed to reproduce, and cell density decreases, cells even detach ones from others, forming holes in the cell layer (figure 4.32).

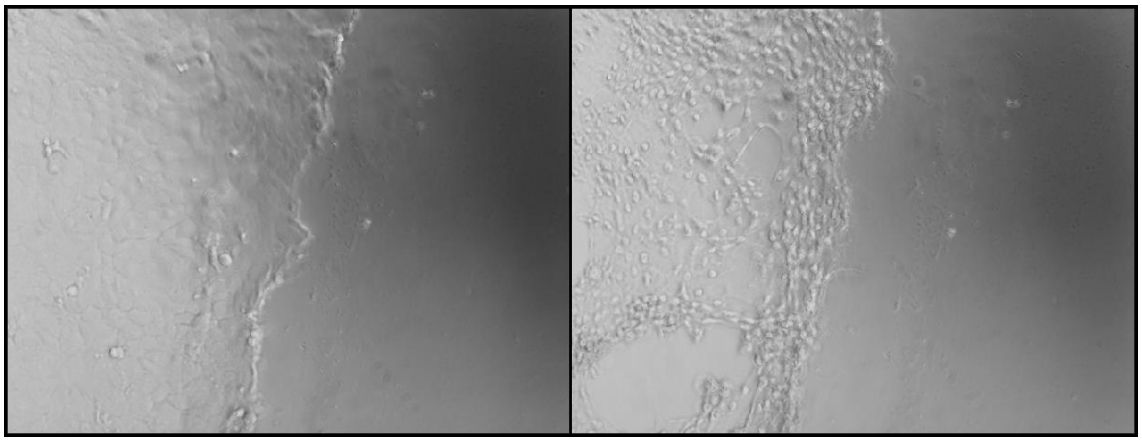

Figure 4.32. Cell progression under – 500 mV. Initial state (left) and state after 24 hours (right).

Quantitative analysis (430 pictures analyzed)**:**

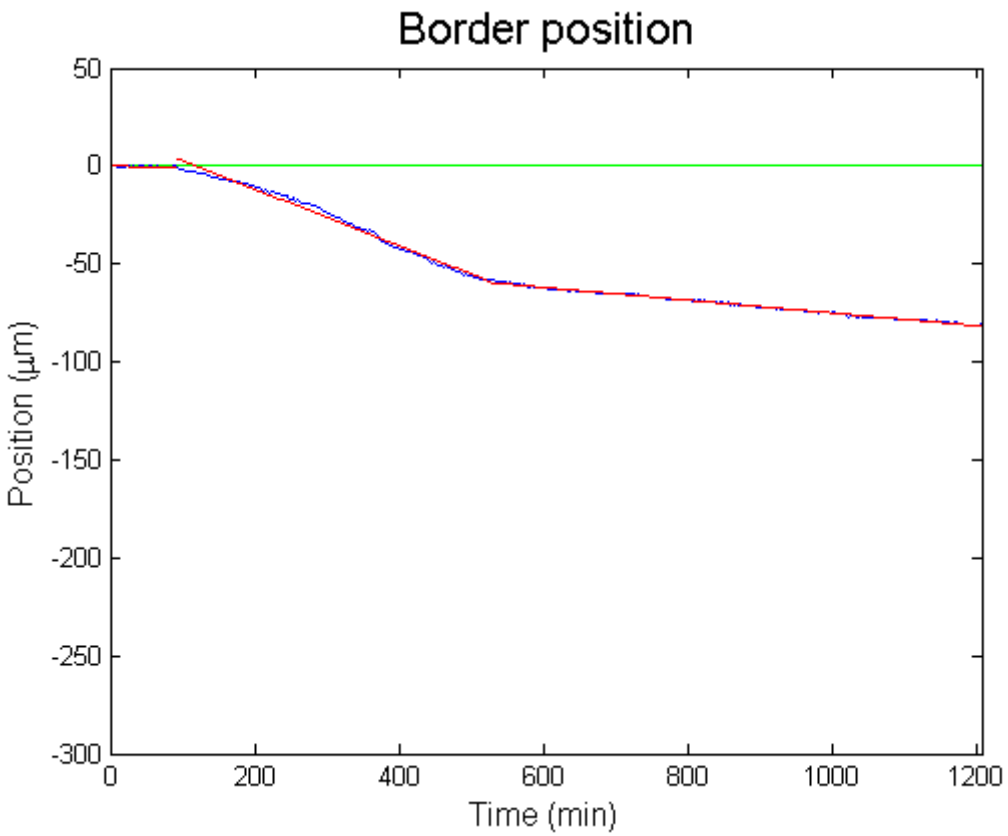

Figure 4.33. Evolution of the cells' border (blue) and three stages linear approximation (red) for experiment 22.

$p_1 = -0.0014t_1 - 0.1115$; $p_2 = -0.1445t_2 + 17.1299$ $p_3 = -0.0327t_3 - 42.3220$

Velocity (from t=0 to t=190) = - 0.001 µm/min.
Velocity (from t=190 to t=705) = - 0.145 µm/min.
Velocity (from t=705) = - 0.033 µm/min.

5. CONCLUSIONS AND FUTURE WORK

There are two main conclusions that can be extracted from the experiments performed. During the wound healing process voltages appear between the wound itself and the surrounding zones. Applying potential differences during wound healing affects the cellular behavior of the cells that are around the wound. Once these two facts have been confirmed, it has been tried to determine whether those phenomena follow a deterministic behavior and can be quantitatively modeled.

Regarding the measuring experiments, it seems that the voltages generated within areas of the same region (being a region the wound zone and different regions the surrounding zones with cell presence) are negligible (figure 5.1). The potential has also been measured to be higher inside the wound compared to the one on the cellular region (figure 5.1). This observation agrees with previous experiments [15], because the cells used are keratinocytes, which are found on the external layer of the skin, the place observed to have the positive pole in the middle of the wound.

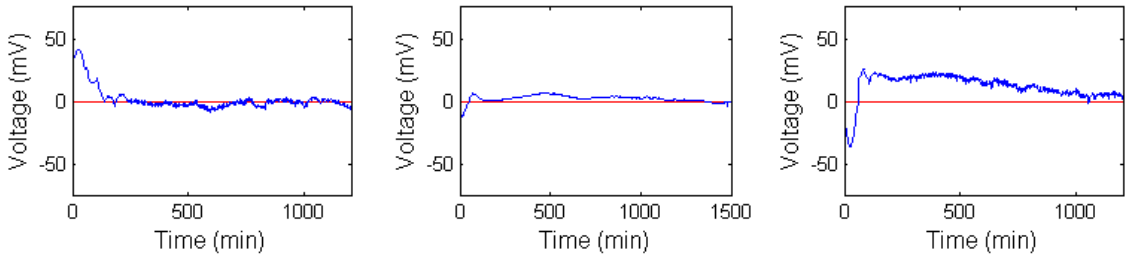

Figure 5.1. Voltages measured between regions around the wound. The potential difference between two points both in the cellular region (left), except for an initial peak, probably due to small scratches performed during wire placing, is negligible. The voltage measured inside the wound (center) is also negligible. The potential difference between the center of the wound and the cellular region (right) is positive (higher potential in the center of the wound) except for an initial reversed peak associated to the initial recessive stage in which cells go away from wound center for a little while.

Further steps within measuring experiments should involve determining the size of the electric field associated to the voltage generated. It is not clear how far the electric field extends from the wound border, although some experiments show that the greater magnitude should be placed close to the wound border [12,13]. Establishing the location of the electric field would give information about the changes in potential along the areas close to the wound. Based on the behavior observed until now, the electric field could be fairly linearly approximated, the unknown is the size of the field. To perform such experiments I would suggest a new wire distribution with the four wires in line so the scope of the electric field associated to the measured potential difference can be better described (figure 5.2).

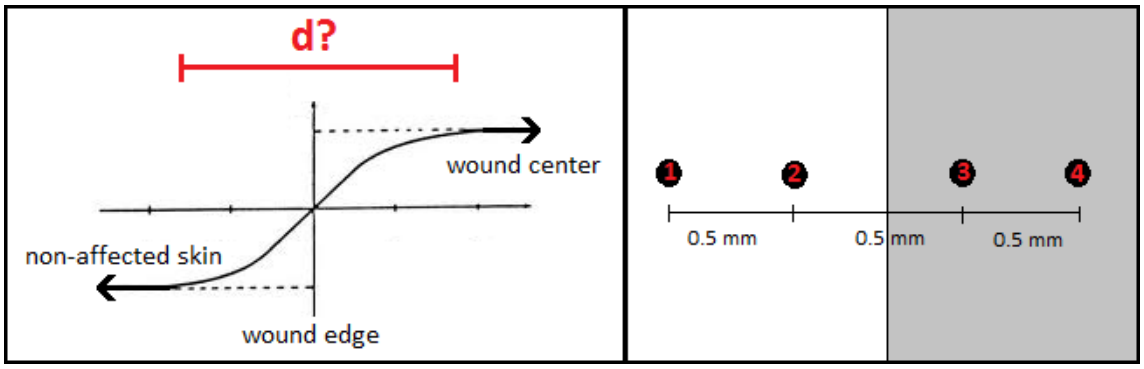

Figure 5.2. Electric field close to the wound. On the left, a schematic approximation of the generated electric field after injury on a keratinocyte monolayer (wound center has higher potential than cell region). On the right, the suggested wire distribution to determine the unknown d.

Talking now about the induction experiments, the behavior of the cells as a function of the voltage induced seems to develop different characteristics within different ranges of voltage (figure 5.3):

- Negative voltages (lower potential in the wound): three stages approximation
  - – 500 mV: no movement initially, after 90 min cells start moving away from wound in two different stages, faster for about 7 hours and then slower.
  - - 300 mV: cells move toward wound center at three different speeds, from faster to slower.

- Range from 0 to 100/150 mV: one stage approximation
  - Cells move towards wound center for the whole range.
  - Velocity seems to increase as voltage increase.

- Range from 150/200 to ~400 mV: two stages approximation
  - Cells move towards wound center initially faster, then, after about 10 hours, slower.
  - As voltage increases, velocity in both stages seems to decrease.

- Voltages higher than ~400 mV: two stages approximation
  - Initially the cells move towards wound center, but they stop and move away from wound center.
  - As voltage increases, the first stage is reduced in time:
    for 500 mV it takes about 8 hours to change direction;
    for 700 mV it takes about 3 hours to change direction.

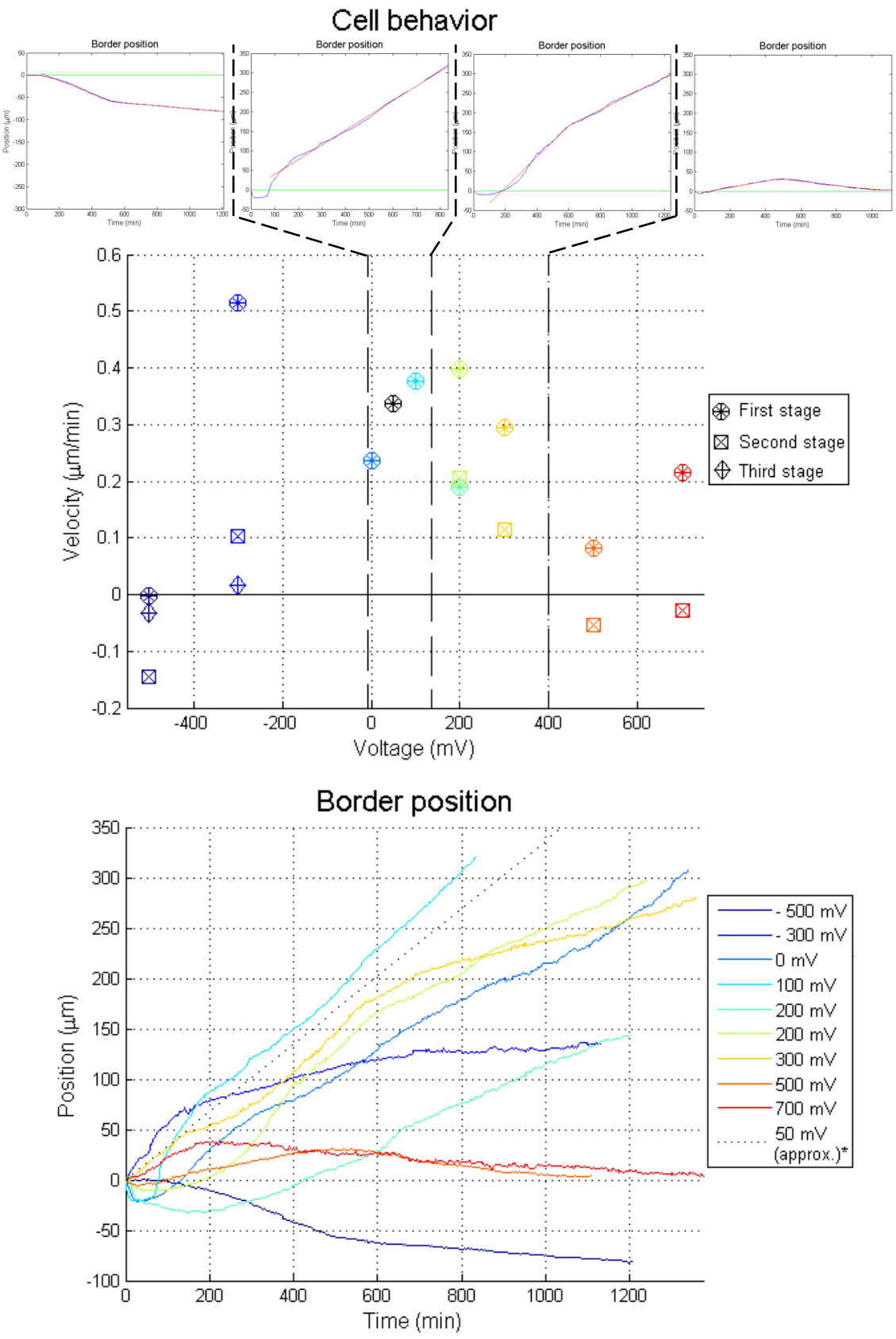

Figure 5.3. Cellular behavior as a function of voltage induced. On top, the change on cell behavior during application of different potentials. The graphic below shows the evolution of cell border from all the experiments plotted all together. *The line for 50mV is the linear interpolation between first and last positions of the edge because border detection picture by picture was not possible (experiment 14).

Further research for induction (very related to the proposed for measuring experiments) will be to discover the actual distribution of the electric field caused by the voltage induced. Is the field so localized that changing the distance between the points where the potential is applied while the voltage is kept constant will make no difference? But the most interesting part is found in the modeling of the behavior. More experiments should be performed to determine quantitatively the change on wound healing due to the applied voltage. Repetitively applying the same potential difference is needed to study the consistency of the results and the voltage differences between experiments should be smaller to have more information.

Common to both types of experiments, the main problem found has been the wires setting. The structure designed allowed to hold the wires in place once they were properly located, but while placing the wires some problems arose. The main difficulty was the scratches that the wires yield on the cell layer because they could not be adjusted directly (figure 5.4.A). The placing of the wires has to be done by hand and the wound size is no more than 1 mm, so the wires usually needed to be repositioned several times. The small wounds produced affect measurements and cell behavior. A solution could be a microneedle array [20]. However, the measurements aimed do not need so high precision, what is interesting here is the behavior as a system instead of very accurate punctual measurements. What is more, the fabrication is costly and complex, so it would not be worth to use such a device. But the main reason to discard it is that the design is compact and opaque (figure 5.4.B), so the imaging tracing would not be possible. So the best solution would be maintain the structure initially designed and modify it to decrease the complexity of the placing of the wires and avoid scratching.

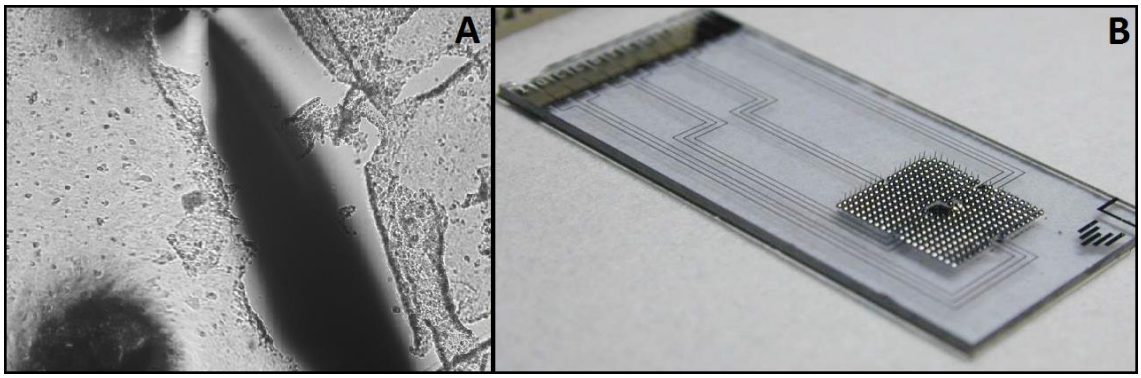

Figure 5.4. Placement of the voltage sensor around the wound. (A) Picture of the wound after wire positioning, some secondary scratches can be appreciated beside the principal wound. (B) Photograph of a completed wound potential measuring device from reference [20].

As a final conclusion it can be said that the work done until now has served to determine how to face the problem and establish a systematic plan to solve it. The ultimate objective, the design of a device to control wound healing, is still very far away, but the results lead to believe that it is an achievable project.

REFERENCES

[1] McLafferty E et al. The integumentary system: anatomy, physiology and function of skin. Nursing Standard. 2010 Apr; 27, 3, 35-42

[2] Diridollou S, Vabre V, Berson M, Vaillant L, Black D, Lagarde JM, Grégoire JM, Gall Y, Patat F. Skin ageing: changes of physical properties of human skin in vivo. Int J Cosmet Sci. 2001 Dec; 23(6):353-62

[3] Black JM, Matassarin-Jacobs E, Luckmann J. Medical-surgical nursing: clinical management for continuity of care (5th ed.). 1997 Jan; 10:0721669506, 13:9780721669502.

[4] Baranoski S, Ayello EA. Wound Care Essentials: Practice Principles. 2006 Sep; 10:1582552746, 13:9781582552743

[5] Foulds IS, Barker AT. Human skin battery potentials and their possible role in wound healing. Br J Dermatol. 1983 Nov; 109:515–22.

[6] Macknight AD, DiBona DR, Leaf A. Sodium transport across toad urinary bladder: a model "tight" epithelium. Physiol Rev. 1980 Jul; 60:615–715.

[7] Larsen EH. Chloride transport by high-resistance heterocellular epithelia. Physiol Rev. 1991 Jan; 71:235–83.

[8] Kunzelmann K, Mall M. Electrolyte transport in the mammalian colon: mechanisms and implications for disease. Physiol Rev. 2002 Jan; 82:245–89.

[9] Du Bois-Reymond E. Vorläufiger Abriss einer Untersuchung uber den sogenannten Froschstrom und die electomotorischen Fische. Ann Phys Chem. 1843 ; 58:1–30.

[10] Borgens RB, Vanable Jr JW, Jaffe LF. Bioelectricity and regeneration: large currents leave the stumps of regenerating newt limbs. Proc Natl Acad Sci USA. 1977 Oct; 74:4528–32.

[11] Illingworth CM, Barker AT. Measurement of electrical currents emerging during the regeneration of amputated finger tips in children. Clin Phys Physiol Measure. 1980 Feb; 1:87.

[12] Reid B, Song B, McCaig CD, Zhao M. Wound healing in rat cornea: the role of electric currents. FASEB J. 2005 Mar; 19:379–86.

[13] Reid B, Nuccitelli R, Zhao M. Non-invasive measurement of bioelectric currents with a vibrating probe. Nat Protoc. 2007 Mar;2:661–9.

[14] Zhao M. Electrical fields in wound healing-An overriding signal that directs cell migration. Semin Cell Dev Biol. 2009 Aug; 20(6):674-82.

[15] Nuccitelli R. A role for endogenous electric fields in wound healing. Curr Top Dev Biol. 2003; 58:1-26.

[16] Stump RF, Robinson KR. Ionic current in Xenopus embryos during neurulation and wound healing. Prog Clin Biol Res. 1986 Jan; 210. 223-30.

[17] Chiang M., Cragoe EJ Jr, Vanable JW Jr. Intrinsic electric fields promote epithelization of wounds in the newt, Notophthalmus viridescens. Dev Biol. 1991 Aug; 146, 377-385.

[18] Sta Iglesia DD, and Vanable JW Jr. Endogenous lateral electric fields around bovine corneal lesions are necessary for and can enhance normal rates of wound healing. Wound Repair Regen. 1998 Nov; 6, 531-542.

[19] Zhao M, Song B, Pu J, Wada T, Reid B, Tai G, Wang F, Guo A, Walczysko P, Gu Y, Sasaki T, Suzuki A, Forrester JV, Bourne HR, Devreotes PN, McCaig CD, Penninger JM. Electrical signals control wound healing through phosphatidylinositol-3-OH kinase-gamma and PTEN. Nature. 2006 Jul; 442:457–60.

[20] Mukerjee EV, Isseroff RR, Nuccitelli R, Collins SD, Smith RL. Microneedle array for measuring wound generated electric fields. Conf Proc IEEE Eng Med Biol Soc. 2006 Feb; 1:4326-8.

ANNEX: Design of the Piece for Wires Fastening